HAW HAMBURG

Bachelor Thesis

Dinda Andiani Putri

Comparing Modes of Transportation with an Improved Karman-Gabrielli Diagram

Fakultät Technik und Informatik
Department Fahrzeugtechnik und
Flugzeugbau

Faculty of Engineering and Computer Science
Department of Automotive and
Aeronautical Engineering

Dinda Andiani Putri

Comparing Modes of Transportation with an Improved Karman-Gabrielli Diagram

Bachelorarbeit eingereicht im Rahmen der Bachelorprüfung

im Studiengang Flugzeugbau
am Department Fahrzeugtechnik und Flugzeugbau
der Fakultät Technik und Informatik
der Hochschule für Angewandte Wissenschaften Hamburg

Erstprüfer: Prof. Dr.-Ing. Dieter Scholz, MSME
Zweitprüfer :   Prof. Dr.-Ing. Martin Wagner

Abgabedatum: 20.04.2023

Any further request may be directed to:
Prof. Dr.-Ing. Dieter Scholz, MSME
E-Mail see: http://www.ProfScholz.de

This work is part of:
Digital Library - Projects & Theses - Prof. Dr. Scholz
http://library.ProfScholz.de

This report is deposited and archived:
- Deutsche Nationalbiliothek (http://www.dnb.de)
- Repositorium der Leibniz Universität Hannover (http://www.repo.uni-hannover.de)
- Internet Archive (http://archive.org), item: ttps://archive.org/details/TextPutri.pdf

This report has associated published data in Harvard Dataverse:
https://doi.org/10.7910/DVN/INTM5L

Name of student

Dinda Andiani Putri

Title of the report

Comparing Modes of Transportation with an Improved Karman-Gabrielli Diagram

Abstract

Purpose – To find, how passengers and freight transport efficiency depends on vehicle cruise speed. Based on the Karman-Gabrielli Diagram, four new diagrams are investigated. Plotted is a) the lift-to-drag ratio (weight-to-drag ratio) versus cruise speed. b) Vehicle weight is replaced by the weight of the payload. c) Plotted is the inverse of energy consumption per payload and range versus cruise speed. d) Energy consumption is replaced by primary energy.

Methodology – For each of the four new diagrams and for each considered means of transport, the governing equations are derived or obtained from literature. Data is collected and the diagrams are plotted. Results are discussed based on new figures of merit visualized in the form of straight iso-lines in the log-log plot. With normal axis the straight lines turn into a typical Pareto fronts.

Findings – Faster cruise speed of a vehicle is associated with reduced efficiency. More meaningful results are obtained if vehicle weight is replaced by the weight of the payload. Even better, if energy consumption is used or primary energy consumption compared to a slower vehicle. Freight ships are the best in fuel economy. The best compromise between fuel consumption and speed may be achieved by the hyperloop.

Research Limitation – This paper includes only a selection of vehicles from each category due to limited data accessibility.

Practical Implications – The Karman-Gabrielli Diagrams enable transportation users to make decisions regarding the most suitable mode of transport, considering various factors such as speed, economy, and environmental impact.

Originality – This seems to be the first report that extends the Karman-Gabrielli Diagram in such a way and proposes new transport figures of merit.

Name des Studierenden

Dinda Andiani Putri

Thema der Bachelorarbeit

Comparing Modes of Transportation with an Improved Karman-Gabrielli Diagram

Stichworte

Luftfahrt, Aerodynamik, Luftwiderstand, Flugzeug, Geschwindigkeit, Nutzlasten, Energieverbrauch, Transport, Fahrzeug

Kurzreferat

Zweck – Es soll ermittelt werden, wie die Effizienz des Personen- und Güterverkehrs von der Fahrgeschwindigkeit abhängt. Auf der Grundlage des Karman-Gabrielli-Diagramms werden vier neue Diagramme untersucht. Dargestellt ist a) das Verhältnis von Auftrieb zu Luftwiderstand (Verhältnis von Gewicht zu Luftwiderstand) in Abhängigkeit von der Reisegeschwindigkeit. b) Das Fahrzeuggewicht wird durch das Gewicht der Nutzlast ersetzt. c) Dargestellt ist die Umkehrung des Energieverbrauchs pro Nutzlast und Reichweite in Abhängigkeit von der Reisegeschwindigkeit. d) Der Energieverbrauch wird durch Primärenergie ersetzt.

Methodik – Für jedes der vier neuen Diagramme und für jedes betrachtete Transportmittel werden die maßgeblichen Gleichungen abgeleitet oder aus der Literatur entnommen. Es werden Daten gesammelt und die Diagramme aufgezeichnet. Die Ergebnisse werden auf der Grundlage neuer Kennzahlen diskutiert, die in Form von geraden Iso-Linien im Log-Log-Diagramm dargestellt werden. Bei normaler Achse gehen die Geraden in typische Pareto-Fronten über.

Ergebnisse – Eine höhere Reisegeschwindigkeit eines Fahrzeugs ist mit einer geringeren Effizienz verbunden. Aussagekräftigere Ergebnisse werden erzielt, wenn das Fahrzeuggewicht durch das Gewicht der Nutzlast ersetzt wird. Noch besser ist es, wenn der Energieverbrauch oder der Primärenergieverbrauch im Vergleich zu einem langsameren Fahrzeug herangezogen wird. Frachtschiffe sind am sparsamsten im Kraftstoffverbrauch. Der beste Kompromiss zwischen Treibstoffverbrauch und Geschwindigkeit kann durch den Hyperloop erreicht werden.

Grenzen der Anwendbarkeit – Aufgrund der begrenzten Datenverfügbarkeit wird in diesem Dokument nur eine Auswahl von Fahrzeugen aus jeder Kategorie berücksichtigt.

Bedeutung für die Praxis – Die Karman-Gabrielli-Diagramme ermöglichen es den Verkehrsteilnehmern, unter Berücksichtigung verschiedener Faktoren wie Geschwindigkeit, Wirtschaftlichkeit und Umweltverträglichkeit eine Entscheidung für das am besten geeignete Verkehrsmittel zu treffen.

Originalität – Dies scheint der erste Bericht zu sein, der das Karman-Gabrielli-Diagramm auf diese Weise erweitert und neue, wertvolle Verkehrszahlen vorschlägt.

Comparing Modes of Transportation with an Improved Kármán-Gabrielli Diagram

Task for a *Bachelor Thesis*

Background

Start of the considerations is:

> GABRIELLI, Giuseppe, VON KARMAN, Theodore, 1950: What price speed? Specific power required for propulsion of vehicles. *Mechanical Engineering,* vol. 72 (1950), no. 10, pp. 775-781. Available from: https://perma.cc/5FZH-YGTR.

Three parameters are collected for each mode of transportation: total weight ($W = mg$), max. power (P) and max. speed (V). $P/(W V)$ is called "specific power". The idea was revisited in 2005 (https://perma.cc/43XQ-BJRW). Now $P/(W V)$ is called "specific resistance". The concept is discussed further e.g. on Wikipedia. Critique of the "Kármán-Gabrielli Diagram" (KG Diagram):

- Only the percentage of power should be considered which is used in cruise.
- Cruise speed should be used not maximum speed.
- Payload should be used instead of total mass.
- Instead of shaft power and speed, energy (fuel) consumption should be used, or even better, primary energy consumption.

Another change to the original publication from 1950: The inverse is used in the KG Diagram: $(W V)/P = W/D = L/D$, with lift (L) and drag (D) we get the glide ratio (L over D), well known in aviation. L/D or W/D is an efficiency to carry weight. In this new way, the KG Diagram may be plotted like this.

The plot shows a straight line in the log-log-plot from top left to bottom right. In a normal plot this line is a hyperbola, which resembles a Pareto front. High speeds result in reduced efficiency. Apparently, you cannot have both. A straight line in the log-log-plot can be drawn through each point, characterizing a vehicle.

Every L/D can be calculated from $L/D = a_{L/D}/V$. In this equation $a_{L/D}$ is a new performance parameter $a_{L/D} = L/D\ V$ (in m/s) that combines the benefits of efficiency and speed. Every vehicle can be assigned such new "transport figure of merit". Two vehicles on the same line

have the same "transport figure of merit". The underlying (philosophical) assumption is: The "transport figure of merit" is the same, if we (e.g.) double speed, while efficiency is halved.

Note also that Specific Air Range, $SAR = L/D \ V/(c \ g) \cdot 1/m$ is the inverse of fuel consumption for jet aircraft (c is the thrust-specific fuel consumption, m is the aircraft's mass). $L/D \ V/(c \ g)$ has the units of meter (m). It is called Breguet factor and is the range of an aircraft that has (unrealistic) 63.2% of its mass at take-off assigned to fuel.

Moreover, $P/(W \ V)$ with $V = s/t$ can also be understood as a proxy of $(P \ t)/(s \ W)$, which can be understood as energy (or fuel) consumption (per distance and) per weight. We plot the inverse of this energy consumption, E per distance and payload. In this way the diagram looks the same as before with L/D. We know, one form of energy (e.g. electricity) cost more than another form of energy (e.g. kerosene). Basically, we pay not for energy, but for "useful" energy, which can be described by exergy. Alternatively, we calculate primary energy from the vehicle's energy requirement. In this case, the "transport figure of merit" follows from $(s \ m_{PL})/E = a_E / V$. In this equation $a_E = (s \ m_{PL})/E \cdot V$ is another form of the "transport figure of merit" now expressed in second (s). This converts speed in m/s into the inverse of energy per distance and payload, given in mkg/J. Investigation could go from energy to emissions or alternatively to operating costs. Speed and energy consumption could be based on their maximum values in the diagram to eliminate scaling effects. In this way, it shows a nonpreferenced "transport figure of merit". If weighting factors k for relative $(s \ m_{PL})/E$ and 1-k for relative V are introduced to express preference for high speed or low energy consumption ($0 \leq k \leq 1$), an a priory linear scaling to express preference is introduced.

As speed increases, so does primary energy. This means, we have to pay for the energy to reach the desired speed. This is the answer to the original question: "What price speed?". We find, some modes of transportation are faster, some consume less energy and some have a higher "transport figure of merit". It is a bicriteria optimization more generally treated as multi-objective optimization.

Task
Illustrate what is explained in the Background. Using the "transport figure of merit", which modes of transportation are better in general? Which in aviation? These are the subtasks:

- Recall systematically the development and reception in literature of the Kármán-Gabrielli Diagram. Look at its various performance parameters (specific power, specific resistance, efficiency to carry weight, energy consumption, primary energy consumption) and related fundamental equations.

- Consider different modes of transportation: On the road (walking, biking, horse, car, truck, ...), on tracks, in the air, on water, and in pipelines. In aviation, consider at best all classes under "Aeronautics/Aircraft" (fixed-wing aircraft – divided by cruise speed and propulsion principle, rotorcraft, lighter than air, unpowered flight). For each mode,

show required equations and considerations to determine power, drag, vehicle and payload mass, energy (fuel) consumption, and primary energy consumption.

- Collect values for all required parameters for each mode of transportation. Show and discuss possible sources of information.
- Plot all mentioned KG Diagrams and calculate the "transport merit" in various forms for all modes of transportation.
- Discuss the results.

The report has to be written in English based on German or international standards on report writing.

Table of Contents

List of Figures

List of Tables

List of Symbols

A_f	Frontal area
A	Aspect ratio
a_E	Transport figure of merit in terms of inverse of primary energy per payload and range
$a_{L/D}$	Transport figure of merit in terms of lift-to-drag ratio
a	Speed of sound
b	Wing span
c	Thrust-specific fuel consumption
c_{D0}	Zero-lift drag coefficient
c_d	Drag coefficient
C_A	Incremental resistance coefficient
C_{AA}	Air resistance coefficient
C_C	Charing crew fees
C_{DOC}	Direct operating cost
C_F	Frictional resistance coefficient
C_{FEE}	Fees and charges
C_M	Maintenance cost
C_T	Total resistance coefficient
D	Drag
D_0	Zero-lift drag
E_{prim}	Primary energy consumption
E	Energy consumption
H_L	Heating value
$\frac{L}{D}$	Lift-to-drag ratio
$\left(\frac{L}{D}\right)_{pl}$	Lift-to-drag ratio regarding payload mass
L	Lift
L_{pp}	Length between perpendicular
M	Mach number
m_{CO2}	Carbon dioxide mass
m_{CO2e}	Equivalent carbon dioxide mass
m_f	Fuel mass
m_{pl}	Payload mass
m	Vehicle mass
P	Maximum power
R_A	Aerodynamic resistance
R_B	Bearing resistance
R_R	Rolling resistance

R_V	Ship's drag
Re	Reynolds number
S_W	Wing area
S_{wet}	Wetted area
T	Draught
V	Cruise speed
W	Vehicle weight
x_{ff}	Share of fossil fuels in electricity generation

Greek Symbols

Δ	Ship's loaded displacement
Δp	Pressure difference
ε	Specific power
λ	Bypass ratio
∇	Ship's volume displacement
ρ_{air}	Air density

List of Abbreviations

BPR   Bypass Ratio
DOC   Direct Operating Cost
KG   Karman-Gabrielli
MTOW Maximum Take Off Weight
SAR   Specific Air Range
SFC   Specific Fuel Consumption

Definitions

Lift-to-drag ratio
"The lift-to-drag ratio (L/D) is the amount of lift generated by a wing or airfoil compared to its drag." (FAA 2023)

Energy consumption
"The amount of energy used by individuals, companies, countries, etc" (Collins 2023a)

Cruising speed
"The speed at which a ship, car, or aircraft travels most efficiently." (Collins 2023b)

Payload
"The load carried by a vehicle exclusive of what is necessary for its operation." (Merriam-Webster 2023a)

Figure of merit
"A numerical quantity based on one or more characteristics of a system or device that represents a measure of efficiency or effectiveness." (Merriam-Webster 2023b)

Specific Air Range
"The distance an airplane travels per unit of fuel consumed." (U.S. EPA 2021)

Maximum take off mass
"The maximum allowable take off mass as stated in the approved certification basis for an airplane type design" (U.S. EPA 2021)

Subsonic
"An airplane that has not been certificated under 14 CFR to exceed Mach 1 in normal operation" (U.S. EPA 2021)

Bulker
"another name for bulk carrier" (Collins 2023c)

Bulk Carrier
"A ship that carries unpackaged cargo, usually consisting of a single dry commodity, such as coal or grain" (Collins 2023c)

Tanker
"A very large ship used for transporting large quantities of gas ot liquid, especially oil" (Collins 2023d)

Container

"Something such as a box or bottle that is used to store things in" (Collins 2023e)

Vessel

"A ship or a large boat" (Collins 2023e)

1   Introduction

1.1   Motivation

The general populace often constrains their understanding of transportation solely to its speed and capacity for conveying goods or individuals to a predetermined destination. Nevertheless, it is imperative to consider additional variables since certain factors may become less efficient and cost-effective at a particular velocity. While particular groups may exhibit a slower pace of movement, they could potentially demonstrate a higher level of efficacy in their actions.

The original Karman-Gabrielli diagram was utilized as a visual aid to depict the power output of a vehicle at a particular speed, thereby illustrating its efficiency at a given velocity. The weight utilized in the original Karman-Gabrielli diagram was solely based on the weight of the vehicle, as the authors lacked precise information pertaining to the useful load of vehicles. Hence, it is imperative to consider the payload mass as a crucial element of a vehicle or the primary objective for utilizing transportation.

Apart from the vehicles load-carrying capacity, energy is another crucial aspect that warrants attention. The utilization of this particular method may potentially result in adverse environmental consequences attributed to the greenhouse gas effect, as well as substantial operational expenses.

1.2   Title Terminology

Terms are defined from the title of the thesis "Comparing Modes of Transportation with an Improved Kármán-Gabrielli Diagram".

Comparing/ to compare
When you compare things, you consider them and discover the differences or similarities between them. (Collins 2023f)

Mode of transport
Method or way of transport or travelling (Collins 2023g)

Mode
A mode of life or behaviour is a particular way of living or behaving. (Collins 2023h)

Transportation
Transportation refers to any type of vehicle that you can travel in or carry goods in. (Collins 2023h)

Compare with:

Means of transport
Any vehicle that you can travel or carry goods in (Collins 2023i)

Mode of transport is a term used to distinguish between different ways of transportation or transporting people or goods. The different modes of transport are air, water, and land transport, which includes rails or railways, road and off-road transport. Other modes also exist, including pipelines, cable transport, and space transport. Human-powered transport and animal-powered transport are sometimes regarded as their own mode, but never fall into the other categories. In general, transportation is used for moving of people, animals, and other goods from one place to another. Means of transport, on the other hand, refers to the transport facilities used to carry people or cargo according to the chosen mode (animal, vehicle, car, airplane, ship, truck, train and so on and so forth). Each mode of transport has a fundamentally different technological solution, and some require a separate environment. Each mode has its own infrastructure, vehicles, transport operators and operations. (Wikipedia 2023a)

Means of transport are transport facilities used to carry people or cargo.
Listed are examples:
- Land: automobiles, bicycles, carriages, pack animals, riding animals, rickshaws, trains, trucks, vehicles, wagons.
- Water: ships.
- Air: aircraft, drone.
- Space: spacecraft.
- Pipeline: pipes, pneumatic tubes.
(Wikipedia 2023b)

As such, this report distinguishes various modes of transport(ation). For each of it, various means of transport are compared with engineering methods. This is done specifically with several forms of an improved Kármán-Gabrielli Diagram.

Improved
Having become better in quality. (Collins 2023j)

The Kármán-Gabrielli Diagram is introduced in the next section, where it is also explained, in which way the diagram can be improved.

1.3   Objectives

The purpose of this paper is to discuss "What price speed?", so that the analysis of the carrying capacity of the vehicle and its energy consumption shall be per performed with the correlation of the cruising speed.

The original Karman-Gabrielli diagram shall be improved, where the lift-to-drag ratio shall be utilized in place of specific resistance, and cruising speed is used in place of maximum speed, which are two of the key characteristics of the diagram that change from those used in prior articles.

This paper will also present several diagrams, among which the most important are:
- Karman-Gabrielli diagram
- Karman-Gabrielli diagram with respect to payload mass
- Inverse of primary energy consumption per payload and range

From the diagrams, the transport figure of merit for several vehicle types, including aerial vehicles, terrestrial vehicles, marine vehicles, and pipeline vehicles, in terms of lift-to-drag ratio a_{LD} and primary energy a_E shall be performed. The aerial vehicles will be then analysed using the Pareto-Front approach.

1.4   Literature

The following sources give the knowledge foundation for this thesis:

- Gabrielli 1950, *"What Price Speed?"*, was the first publication to propose the theory of Karman-Gabrielli diagram.

- Trancossi 2015, *"What price speed? A critical revision through constructal optimization of transport modes"*, revised the original Karman-Gabrielli diagram by discussing about the other approaches from several theories and discussing in terms of relative energy efficiency.

- Teitler and Proodian 1980, *"What Price Speed? , Revisited"*, explained that the emipircal parameter A in the equation proposed by Gabrielli 1950 can be violated by several factors of technological progress, such as a decrease in drag or a decrease in gross weight due to advances in mechanics or material structure.

- The Railway Research Group 2005, *"What Price Speed - Revisited"*, provides a brief explanation of some of the advances in technology over time, especially modern vehicles, that may have influenced the original theory.

- Wikipedia 2023c, *"Diagramme de Gabrielli – von Karman"* given by Prof. Scholz, represents the idea of revising the Karman-Gabrielli diagram using the approach of lift-to-drag ratio.

- Scholz 2022b, lecture notes *"Flight Mechanics"* at the Department of Automotive and Aeronautical Engineering of the Hamburg University of Applied Science (HAW Hamburg), where theoretical understanding regarding drag of aircraft, car, train and ship, as well as specific air range acquired.

- Scholz 2019, (presentation) *"Limits to Principles of Electric Flight"* Slide 57, provides information regarding primary energy and CO2 emission for vehicle powered with kerosene and battery.

- Scholz 2015, lecture notes *"Aircraft Design"* at the Department of Automotive and Aeronautical Engineering of the Hamburg University of Applied Science (HAW Hamburg), has information regarding Direct Operating Cost.

1.5   Structure of the Work

Chapter 2   recalls the development and reception in the literature of the Karman-Gabrielli Diagram.

Chapter 3   explains the required equations and considerations to determine drag, vehicle and payload mass, energy (fuel) consumption, and primary energy consumption for different modes of transportation.

Chapter 4   examines values for all required parameters for each mode of transportation. The parameters are displayed in tables.

Chapter 5   discusses the result of the Karman-Gabrielli Diagram in regard to the „transport merit" of different modes of transportation and its emission.

The Excel table to this thesis and further data can be found at Harvard Dataverse:
https://doi.org/10.7910/DVN/INTM5L

2 Karman-Gabrielli Diagram

The Karman-Gabrielli diagram was established in 1950 to calculate the specific power required for vehicle propulsion. The specific power of a vehicle is determined by the ratio of the maximum power needed to propel the vehicle to its weight, as a function of the maximum speed (Gabrielli 1950).

$$\varepsilon = \frac{P}{W \cdot V} \tag{2.1}$$

The weight that was used in (2.1) is vehicle weight, regardless of the payload mass because the author does not have any access to the payload mass data.

The power-to-speed ratio pertains to the tractive force and denotes the utilization of the entire power for propulsion while achieving a propulsive performance of 100 percent. The tractive force encompasses not only the direct drag, but also the drag that is commensurate with the losses incurred by the transmission and propulsive mechanism, in conjunction with the gross weight of the vehicle (Gabrielli 1950). The nomenclature of the Karman-Gabrielli diagram parameter has been modified to specific resistance (Trancossi 2015).
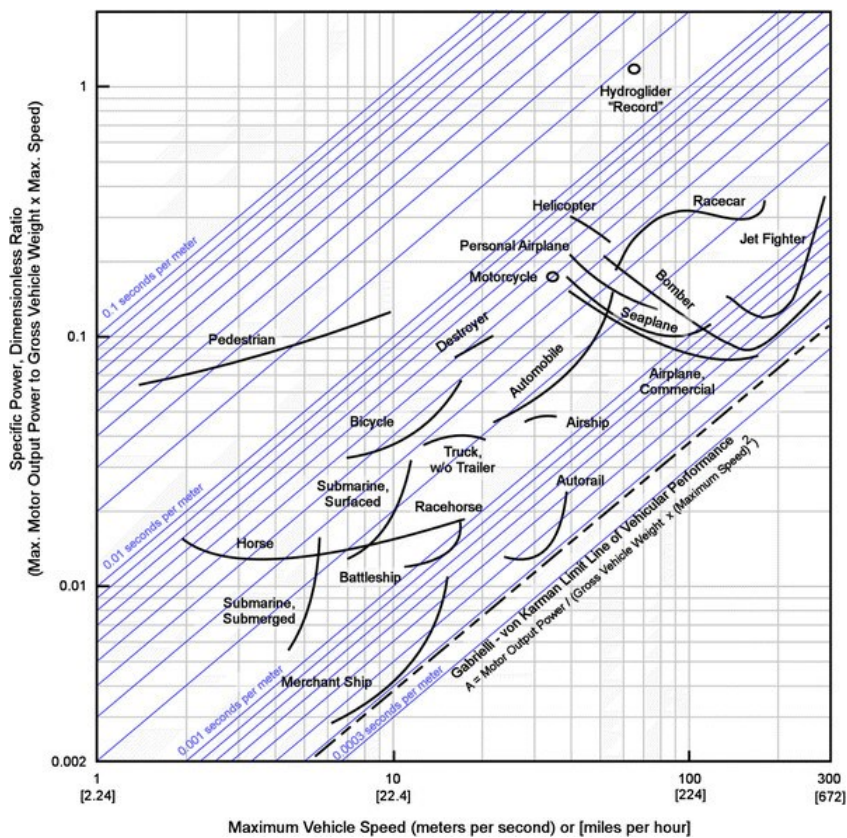
Figure 2.1   The original Karman-Gabrielli graph as presented by Trancossi (2016)

Figure 2.1 depicts the Karman-Gabrielli Diagram with some curves for various modes of transportation and limitation line. Each curve line illustrates the specific power of different vehicle types within the same transportation mode category that has varying maximum speeds. The limit line is denoted by A and considered in Trancossi (2015) as a factor describing an experimental performance limit where A = 0,000175 h/mile. The more closely the curve approaches the line, the more efficient the mode of transportation is relative to others in a certain maximum speed. The merchant ship, train, and aircraft are the three vehicles with the closest curves to the limit line, as seen in Figure 2.1.

A further modification was made to the original 1950 publication, in which the inverse of specific resistance is applied in the Karman-Gabrielli Diagram (Wikipedia 2023c).

$$\frac{W \cdot V}{P} = \frac{W}{D} = \frac{L}{D} \tag{2.2}$$

The lift-to-drag ratio can be calculated with the lift-to-drag ratio in (2.2). It is commonly used in aviation to demonstrate an aircraft's efficiency for carrying capacity. As it is currently inversed, the diagram will appear as shown in Figure 2.2. The plot displays the technological limit running from the top left to the bottom right in the log-log plot. This implies that a vehicle's capacity to carry weight decreases with increasing maximum speed.
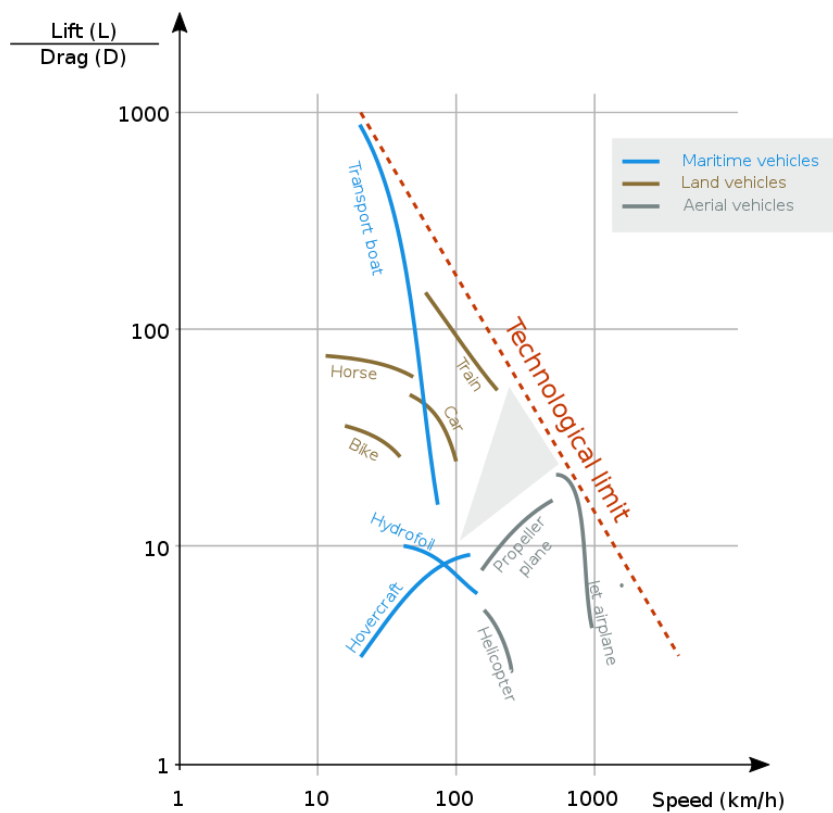
Figure 2.2   The Karman-Gabrielli Graph using L/D approach (Wikipedia 2023c)

Since the glide ratio or lift-to-drag ratio is only commonly used in aviation, the lift over drag for other modes of transport can be calculated using frictional force and weight. Here, the lift is equal to the weight of the vehicle, and the drag could be estimated by using frictional force at cruise speed. For more specific applications in naval architecture, (2.3) can be used (Wikipedia 2023c).

$$\frac{L}{D} = \frac{\Delta}{R_V} \tag{2.3}$$

Δ is the loaded displacement of the ship and R_V is the drag of the ship.

The original Karman-Gabrielli graphic, however, is based on the vehicle's weight, its maximum power, and its maximum speed. Some factors weren't taken into consideration (Wikipedia 2023c), like:

- The amount of power used when traveling at cruising speed.
- The market weight to total weight ratio.
- A lack of analysis of the energy necessary to transport the payload. As result, the graph doesn't give an advantage to carrying more freight or passenger.
- There is no clear indication of the consumption per transported person in the diagram to picture the cost of the transport.
- Whether it is primary or final energy, information is required.

As a result, in this paper, these factors will be considered and then applied to the Karman-Gabrielli diagram. Because the maximum speed is rarely applied in practical cases and the cruising speed is the most frequent, the cruise speed will be used instead of the maximum speed. Primary energy will be applied since the initial consumption of the vehicle should be taken into account rather than what end users really use because it has been dropped due to distribution. And because the transported weight is also important to include in the calculation, the total weight consisting of vehicle weight and payload weight will be considered along with the ratio between payload weight and total weight.

3 Equations for the Modes of Transportation

Various transportation modes can be classified into distinct categories, including aerial vehicles, marine vehicles, terrestrial vehicles, and pipeline transport. The determination of drag, cruising speed, vehicle weight and payload mass, energy (fuel usage), and primary energy consumption varies across different categories. This chapter will provide a detailed explanation of how the combination of drag and mass typically yields the lift-to-drag ratio for various vehicles.

Equally important, the payload mass should be taken into account rather than the overall mass since the focus of this study is solely on a vehicle's capacity to convey people and goods. Determining the ratio between maximum payload mass m_{mpl} and total mass m is necessary since the lift-to-drag defines vehicle's capacity to carry its total mass during cruise. At the end, the ratio of payload mass to total mass is to be multiplied with the lift-to-drag ratio to determine the lift-to-drag ratio regarding payload mass[1] $(\frac{L}{D})_{pl}$. This applies to all vehicles.

$$\left(\frac{L}{D}\right)_{pl} = \frac{m_{pl}}{m} \cdot \left(\frac{L}{D}\right) \tag{3.1}$$

3.1 Air Transport

Aerial vehicles are essentially aircraft that are then classified based on their propulsion system (Gulani 2022).

3.1.1 Subsonic Fixed-Wing Aircraft

An aircraft's objective is to produce a high lift and little drag since high lift allows it to carry more payload. It is measured using the lift-to-drag ratio, which is the ratio of lift to drag. Unfortunately, induced drag also occurs whenever an aerodynamic body produces lift. In order to generate lift at a lower speed, an aircraft must adopt a greater angle of attack, which increases induced drag. However, the induced drag also decreased as the aircraft reached a certain high speed and dropped the angle of attack like to be seen in Figure 3.1. On the other side, there is a second drag known as parasite drag that increases as speed increases. The movement of the airplane against the air causes parasite drag, hence the faster the aircraft travels, the greater the parasite drag. Back to the primary objective, which is to carry as much payload as possible, the maximum lift-to-drag ratio must be accomplished. The maximum lift-

---

[1]   The equation refers to Prof. Scholz's explanation during thesis supervision.

to-drag ratio indicates the aircraft's optimal performance to carry weight and is designed to operate properly at the selected cruising speed in regards of maximizing economy (Wikipedia 2023d).
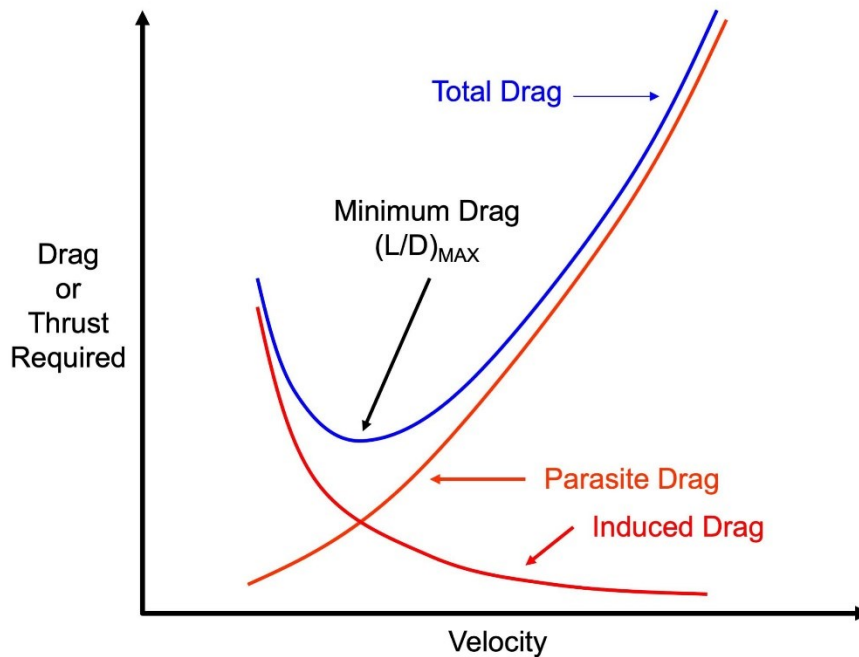
Figure 3.1   The drag and airspeed curve (Code 7700 2023)

The coefficients of lift and drag are denoted as c_L and c_D, respectively. The proportionality between the coefficients' ratio and the lift-to-drag ratio is observed. The utilization of the second approach is preferred due to the complexities involved in determining the lift coefficient at which the aircraft cruises. This approach entails approximating the maximum lift-to-drag ratio or minimum drag (Scholz 2022a).

$$E_{max} = \left(\frac{L}{D}\right)_{max} = k_E \sqrt{\frac{A}{\frac{S_{wet}}{S_W}}} \tag{3.2}$$

According to statistics, the value from k_E could be simplified by classifying different flight lengths as to be shown in Table 3.1.

Table 3.1   The value from k_E according to flight length (Scholz 2022a)

Flight Length	k_E
Short Range	15.15
Medium Range	16.19
Long Range	17,25

The relative wetted area S_{wet}/S_W of several subsonic aircraft can be seen in Figure 3.2.
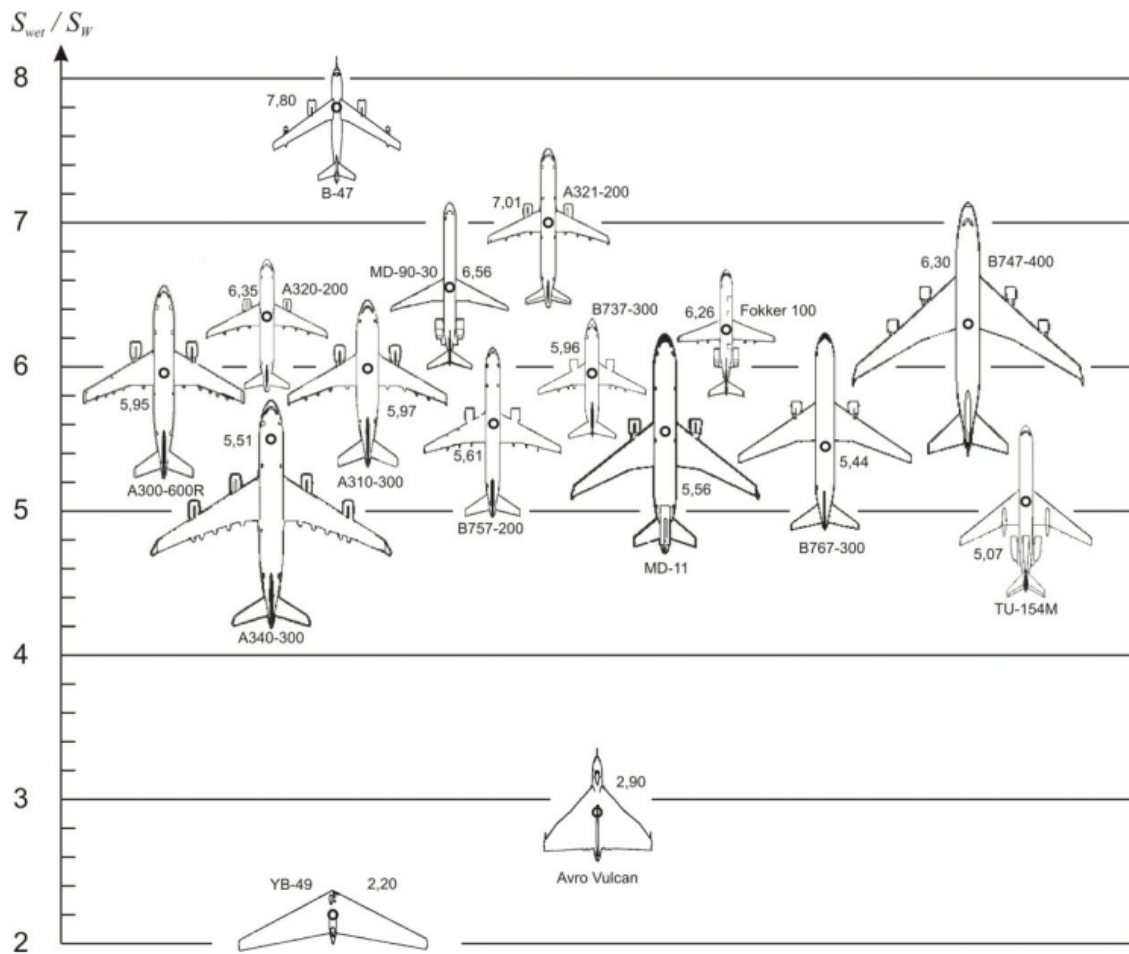
Figure 3.2 Subsonic fixed-wing aircraft relative wetted area S_{wet}/S_W (Scholz 2022a)

The aspect ratio A of the wing is defined as the ratio of the square value of the wingspan b to the wing area S_W.

$$A = \frac{b^2}{S_W} \tag{3.3}$$

The objective is to optimize the payload capacity while taking into account the fuel mass. The maximum take-off weight (MTOW) of an aircraft includes the fuel mass necessary to attain the intended distance.
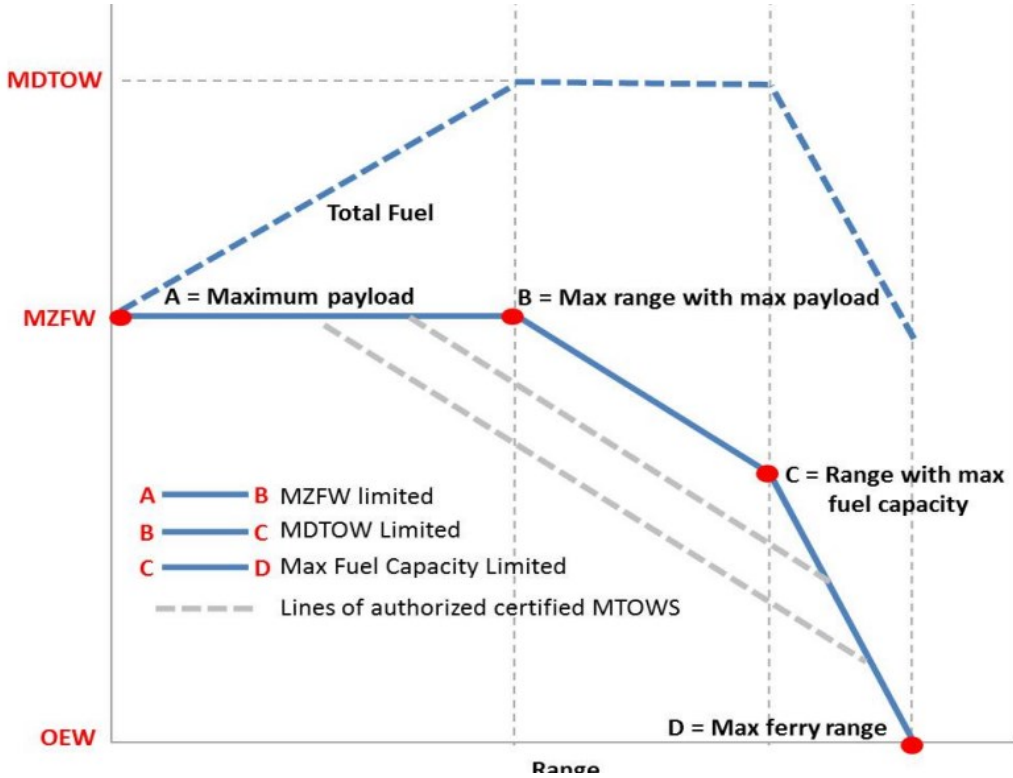
Figure 3.3   Payload-range diagram (Ackert 2013)

The range varies depending on the fuel variety and cargo weight, as shown in Figure 3.3. The payload that can be transported decreases with increasing range. The state of zero fuel weight and maximum payload is shown in the left section. The middle part indicates the maximum take-off weight, where the payload mass and fuel mass can be modified according to the desired range, and the slope in this section define the specific air range (SAR) (Scholz 2022b). SAR for the jet engine can be calculated with:

$$SAR = -\frac{dR}{dm} = \frac{V\,E}{cg} \cdot \frac{1}{m}$$

(3.4)

E is the aircaft lift-to-drag ratio, c is the thrust-specific fuel consumption and m is the take-off mass. To determine the SFC in cruise condition, the data of SFC in cruise from Hammami (2021a) and a simple mathematical method also from Hammami (2021b) of SFC Models from Minimum Mean Square Error will be applied with the input of aircraft engine bypass ratio λ and cruise speed V.

$$c = 3.735 \cdot 10^{-8} \cdot \lambda^{-2.12 \cdot 10^{-3}} \cdot V + 1.65 \cdot 10^{-5} \cdot \lambda^{-0,4}$$

(3.5)

The inverse of SAR is the fuel consumption of the aircraft which then can be defined as fuel mass m_f divided with the distance travelled or range s as to be seen in (3.6). With the correlation to (3.4), the lift-to-drag ratio has an inversely proportional relationship with fuel consumption.

$$\frac{1}{SAR} = \frac{m_f}{s} \tag{3.6}$$

To calculate the energy consumption per distance and payload, the heating value of kerosene H_L should be multiplied by the inverse of SAR from (3.6) and divided by the payload mass m_{pl}.

$$\frac{E}{s \cdot m_{pl}} = \frac{1}{SAR} \cdot \frac{H_L}{m_{pl}} = \frac{m_f \cdot H_L}{s \cdot m_{pl}} \tag{3.7}$$

The primary energy consumption per payload range should be determined instead of only the energy consumption per payload range to know the real energy instead of useful energy by multiplying the efficiency factor 1.1 since aircraft uses kerosene as fuel (Scholz 2019).

$$\frac{E_{prim}}{s \cdot m_{pl}} = 1.1 \cdot \frac{E}{s \cdot m_{pl}} \tag{3.8}$$

3.1.2 Supersonic Fixed-Wing Aircraft

Certainly, a supersonic fixed-wing aircraft has a much faster speed than a subsonic fixed-wing aircraft. To calculate the maximum lift-to-drag, the equation used according to Küchemann (2012) is as follows,

$$\left(\frac{L}{D}\right)_{max} = \frac{3(M+3)}{M} \tag{3.9}$$

Mach number, M is he ratio of speed V to speed of sound a. The formula below is used to determine the Mach number:

$$M = \frac{V}{a} \tag{3.10}$$

a is the speed of sound at a certain altitude. In this paper, the altitude applied is the cruise altitude.

The methodology employed for determining the energy utilization per unit of payload range and the primary energy utilization per unit of payload range is analogous to the one utilized in subsonic fixed-wing airplanes.

3.1.3 Rotorcraft

One of the vehicles that use rotorcraft as a propulsion technology is the helicopter. A helicopter is a rotor-driven, heavier-than-air aircraft with engine-powered rotors.

In order to ascertain the lift-to-drag ratio of the helicopter, (3.11) will be employed, utilizing the input parameters of the helicopter's continuous power P_{cont}, total weight W, and cruising speed V.

$$\frac{L}{D} = \frac{m \cdot V}{P_{cont}} \tag{3.11}$$

The lift-to-drag ratio may also be evaluated by examining the state of the helicopter during autorotation. Autorotation is a state of flight in which the primary rotor system is rotated by the force of relative wind, rather than by the power generated by the engine. Furthermore, in the event of the engine being turned off, the helicopter is capable of executing a secure landing. The pilot is responsible for regulating the aforementioned ratio during the process of autorotation, and a glide ratio of 4:1 is generally regarded as a secure parameter (HighSkyFlying 2023).

The fuel consumption per payload can be calculated by dividing the fuel mass and heating value of kerosene by the helicopter cruise range and payload.

$$\frac{E}{s \cdot m_{pl}} = \frac{H_L \cdot m_f}{R \cdot m_{pl}} \tag{3.12}$$

To obtain the primary energy consumption per payload range, (3.8) of a subsonic fixed-wing aircraft can be used.

3.1.4 Airship

Due to the fact that an airship flies based on buoyancy, it has no induced drag. As the amount of an airship's buoyancy is determined by its volume, a high-altitude airship undoubtedly has a large profile area, which contributes significantly to its profile drag or also categorized as zero lift drag.

Drag is something that will be experienced by any transportation system that is travelling through an air-filled space which is affected by the air density ρ_{air}, cruise speed V, the arbitrary reference area calculated from the volume of the airship S_V, and the coefficient of drag c_{DV}.

$$D_0 = \frac{1}{2} \cdot \rho_{air} \cdot V^2 \cdot c_{DV} \cdot S_V \tag{3.13}$$

Because of the lower air density at higher altitudes, the amount of zero-lift drag decreases as its altitude increases. The airship's normal cruising altitude for LZ-129 Hindenburg is 200 m, which is extremely lower than the fixed-wing aircraft (Grossman 2017).

The arbitrary reference area calculated from the volume of the airship can be approximated according to Hoerner (1965) as follows:

$$S_V = V^{\frac{2}{3}} \tag{3.14}$$

where V is the volume of the airship envelopes.

The drag coefficient c_{DV} can be estimated through the length l and maximum diameter d of the airship (Hoerner 1965).

$$c_{DV} = \left[0.172 \left(\frac{l}{d}\right)^{\frac{1}{3}} + 0.252 \left(\frac{d}{l}\right)^{1.2} + 1.032 \left(\frac{d}{l}\right)^{2.7} \right] \cdot \frac{1}{Re^{\frac{1}{6}}} \tag{3.15}$$

The Reynolds number Re can be calculated using the following formula (Hoerner 1965),

$$Re = \frac{V \cdot l}{\nu} \tag{3.16}$$

Where V is the cruise speed, l is the length of the airship and ν is kinematic viscosity of the air as a function of altitude. Since airships fly at quite low altitude, then it is considered that the kinematic viscosity at sea level equal to $1.46 \cdot 10^{-5}$ m²/s.

The lift to drag ratio can be calculated by dividing the weight of the airship with the drag D_0.

$$\frac{L}{D} = \frac{m \cdot g}{D_0} \tag{3.17}$$

As per the principle of buoyancy, a fluid is capable of generating an upward force that is equal to the weight of the fluid displaced by an object. This is the underlying mechanism responsible for the generation of lift on an object. The utilization of static lift is employed to elevate an airship when it is filled with a lifting gas that possesses a specific weight that is less than that of atmospheric air. The commonly utilized propellants for airships are hydrogen and helium. Compared to hydrogen, helium possesses a higher ignition temperature, rendering it a

safer alternative. However, the acquisition of helium presents challenges due to its scarcity and high cost. Hydrogen's lower density provides increased buoyancy, however, its combustibility is a significant concern (Britannica 2023). The airship utilizes diesel as a propellant for its engine, thereby producing thrust.

3.1.5 Glider

A glider's wings must generate sufficient lift to maintain the glider's weight. The wings produce more lift as the glider travels faster. The wings will provide enough lift if the glider flies quickly enough to keep it in the air. But the glider's body and wings also generate drag, and the quicker the glider is flying, the more drag they generate. A glider needs to produce speed in an alternative way since it has no engine to provide thrust. The glider can fly faster to produce the lift required to carry its weight by angling downward and losing altitude (Brain 2023). The horizontal distance must be divided by the elevation change in order to determine the glide ratio, or L/D, of the glider (NASA 2023). Since it is an unpowered flight, it does not require any fuel or energy to operate.

3.2 Water Transport

Based on experience, a marine vehicle with similar weight as a train is estimated to have less drag than a train (Scholz 2022b).

3.2.1 Bulker, Tanker and Container Vessel

There are a few common resistances to ship propulsion, which include frictional resistance, incremental resistance, air resistance, and residual resistance. To determine the total resistance R_T, it is necessary to first determine the total resistance coefficient C_T for all types of resistance (Kristensen 2017a).

$$C_T = C_F + C_A + C_{AA} + C_R = \frac{R_T}{\frac{1}{2} \cdot \rho \cdot S_W \cdot V^2} \tag{3.18}$$

The frictional resistance coefficient C_F is defined as a parameter related to the surface roughness of the hull, where the frictional resistance R_F is the sum of the tangential stresses

along the wetted surface in the direction of motion and defines by the ITTC-57 formula in Kristensen (2017a) as,

$$C_F = \frac{0.075}{(\log Re - 2)^2} = \frac{R_F}{\frac{1}{2} \cdot \rho \cdot S_W \cdot V^2} \qquad (3.19)$$

The Reynolds number Re calculated by,

$$Re = \frac{V \cdot L_{wl}}{\nu} \qquad (3.20)$$

The kinematic viscosity of water at sea as function of temperature is assumed $1.14 \cdot 10^{-6}$ m²/s at 15°C. The length of a vessel where it is submerged in water is referred to as length of waterline L_{wl}.

The incremental coefficient C_A is the parameter related to ship's surface and using the following expression by Kristensen (2017a).

$$1000 \cdot C_A = 0.5 \cdot \log(\Delta) - 0.1 \cdot (\log(\Delta))^2 \qquad (3.21)$$

The loaded displacement of a ship, denoted by Δ, is a measure of its weight in kg, encompassing the combined mass of the vessel, its cargo, and any necessary operational requirements.

To define the air resistance coefficient C_{AA}, the Table 3.2 is given from for tankers and bulkers.

Table 3.2   Air resistance coefficient for tankers and bulker (Kristensen 2017a).

Vessel Type	$C_{AA} \cdot 1000$
Small tankers	0.07
Handysize tankers	0.07
Handymax tankers	0.07
Panamax tankers	0.05
Aframax tankers	0.05
Suezmax tankers	0.05
VLCC	0.04

The additional resistance brought on by the hull's shape or curvature, viscous pressure resistance, and wave resistance are all components of the residual resistance.

To calculate the total ship resistance, the wetted surface specification is also to be determined. It is normally discovered via a hydrostatic program. Instead, because the source is limited, the estimation approach from Mumford's formula will be used (Kristensen 2017a).

$$S_W = 1.025 \cdot \left(\frac{\nabla}{T} + 1.7 \cdot L_{pp} \cdot T \right) \tag{3.22}$$

L_{pp} and T defined as the length between perpendicular and draught of the ship. The term length between perpendicular refers to the distance measured from the foreside of the stem to the afterside of the rudder post at the vessel's summer loadline. The draft of a vessel refers to the vertical distance between the waterline and the deepest point of the vessel. The volume ship displacement ∇, which is expressed in cubic meters, is the amount of water it moves when it is floating (Gard.no 2012). The dimensions of volume ship displacement ∇ and loaded ship displacement Δ are essentially similar, albeit with distinct unit displays.

With the specification of the square of cruise speed V^2 and water density ρ, the rearrangement of (3.19) results in total resistance.

$$R_T = \frac{1}{2} \cdot C_T \cdot \rho \cdot S_W \cdot V^2 \tag{3.23}$$

All the above calculations aimed at obtaining total resistance can be calculated with the Excel table from Kristensen (2017b). Details about ship dimensions and total resistance during cruise of several types of tanker, bulker and container vessel are provided by inputting ship's maximum deadweight tonnage and cruise speed on the Excel table form Kristensen (2017b).

As shown in Figures 3.4 and Figure 3.5, the maximum dead weight tonnage of the vessel should be entered to specify the type of bulker or tanker. The maximum dead weight tonnage is a measurement of the ship's carrying capacity, which includes cargo on board, fuel, ballast water, fresh water, crew, and provisions for the crew, but excludes the ship's own weight (Cogoport 2023).

Ship data	Units	Deafault
Bulker type: Small (< 10000 DWT) - Handysize (10000 - 25000 DWT) - Handymax (25000 - 55000 DWT) - Panamax (55000 - 85000 DWT) - Capesize (85000 - 200000 DWT) - VLBC (>200000 DWT)	-	Small bulk carrier
Maximum deadweight	tons	7000

Figure 3.4   Bulker types and its dead weight tonnage.

Ship data	Units	Deafult values
Tanker type: Small (< 10000 DWT) - Handysize (10000 - 25000 DWT) - Handymax (25000 - 55000 DWT) - Panamax (55000 - 80000 DWT) - Aframax (70000 - 120000 DWT) - Suezmax (120000 - 200000 DWT) - VLCC (200000 - 330000 DWT)	-	Small tanker
Maximum deadweight	tons	7000

Figure 3.5   Tanker types and its dead weight tonnage.

The loaded displacement Δ of the vessel in kg was then divided with the total resistance R_T to determine the lift-to-drag of the vessel (Wikipedia 2023c).

$$\frac{L}{D} = \frac{\Delta \cdot g}{R_T}$$

(3.24)

The most popular fuel for commercial vessels is HFO, or heavy fuel oil. Thus to determine fuel consumption or energy consumption, the caloric value of both the primary and auxiliary engines must be considered. Each caloric value should be multiplied by the hourly oil consumption, and the sum of the two will equal the hourly energy demand. When the energy demand per hour is divided by speed and payload mass, the energy demand per weight and distance may be calculated. The information about the energy consumption is also provided in Excel table from Kristensen (2017b). In order to determine the energy consumption of a vessel, it is necessary to calculate the product of the oil consumption of both the main engine $\frac{m_{oil,maimn\ engine}}{t}$ and auxiliary engine $\frac{m_{oil,auxilary\ engine}}{t}$ while at sea, and the corresponding heating value H_L.

$$\frac{E}{t} = \frac{m_{oil,auxilary\ engine}}{t} \cdot H_L + \frac{m_{oil,main\ engine}}{t} \cdot H_L$$

(3.25)

To determine the energy consumption per payload and range, (3.26) is employed, wherein the energy consumption is divided by the product of the cruise speed V and payload mass m_{pl}.

$$\frac{E}{s \cdot m_{pl}} = \frac{E}{t} \cdot \frac{1}{V \cdot m_{pl}}$$

(3.26)

3.2.2   Cruise Ship

Cruise ships are designed to carry more passengers than freight, and some are even designed for only recreational purposes. As a result, the weight of each passenger and their luggage will be assumed as the payload. An average passenger weighs 88 kg according to Berdowski (2009) and the checked baggage weight may vary for each type of transport. As an example, the baggage allowance per passenger for Norwegian Cruise Line is maximum 50 pound or equal to 22 kg (NCL 2023).

Theoretically, the calculation method to determine the resistance of passenger ships is similar to bulker and tanker and container vessel. However, in slow ship designs, the frictional resistance can account for 80% of total resistance, then it is decided to only include the

frictional resistance for passenger ship as in (3.19) and (3.23). The lift-to-drag ratio will be determined using (3.24).

Since the ship burns diesel fuel, if the information is given as fuel consumption in kg/m, it must be multiplied by the heating value of diesel H_L, divided by the mass of the payload m_{pl} to produce energy consumption per payload and range,

$$\frac{E}{s \cdot m_{pl}} = \frac{m_f}{s} \cdot \frac{H_L}{m_{pl}}$$

(3.27)

Then it should be multiplied by a factor of 1.1 to obtain primary energy per payload and range.

$$\frac{E_{prim}}{s \cdot m_{pl}} = 1.1 \cdot \frac{E}{s \cdot m_{pl}}$$

(3.28)

3.3 Land Transport

3.3.1 Car, Truck and Bus

For short distance travel, car, truck and bus are frequently used. The capacity can vary, it can run on gasoline or diesel, and modern cars can even run on electricity.

Rolling resistance and aerodynamic drag are the drag factors for these vehicles. The vehicles' design, particularly the frontal area A_f, has a significant impact on the amount of aerodynamic drag R_A. The greater the surface area, the greater the aerodynamic resistance.

$$R_A = \frac{1}{2} \cdot \rho_{air} \cdot c_d \cdot A_f \cdot V^2$$

(3.29)

A dimensionless parameter known as the drag coefficient c_d is used to measure an object's resistance to motion in a fluid environment like air or water. Utilizing a wind tunnel, it is possible to experimentally determine the true drag coefficient (Kmet 2022).

The rolling resistance of the vehicle R_R is determined by the vehicle's weight $m \cdot g$ and the surface roughness of the track which has the parameter of rolling friction coefficient μ_R as seem om Table 3.3.

Table 3.3   Rolling friction coefficient (Scholz 2022b)

Track	μ_R
Car tires and asphalt	0.015
Car tires and earth way	0.05

Therefore, the rolling resistance R_R equation can be expressed as follows:

$$R_R = m \cdot g \cdot \mu_R \tag{3.30}$$

At the end, the total resistance is the sum of aerodynamic drag and the rolling resistance.

$$R_T = R_A + R_R \tag{3.31}$$

The weight of the car and the load $m \cdot g$ must be divided by the total resistance R_T in order to determine the lift-to-drag ratio of the vehicle.

$$\frac{L}{D} = \frac{m \cdot g}{R_T} \tag{3.32}$$

Gasoline or diesel is the predominant fuel for these vehicles. The fuel consumption is measured in liters per 100 km. Alternatively, gallons per 100 miles in nations that adhere to the imperial system. The amount of energy required to travel 100 km in an electric vehicle is stated in kilowatt-hours, as the vehicle does not consume gasoline but rather draws its power from a battery. There is an additional characteristic for automobiles that is referred to as the fuel economy. This criterion determines how far the vehicle is capable of traveling on a certain quantity of gasoline, making it equivalent to the opposite of how fuel consumption is defined, which normally defined in imperial system as miles per gallon or meter per joule in metric with one gasoline galloon equal to 33.41 kWh or 120.276 MJ. In order to determine the primary energy of a conventional car, it is necessary to multiply the energy consumption per unit payload and range by a factor of 1.1. Meanwhile, for an electric car, the energy consumption per unit payload and range should be multiplied by a factor of 2.1.

3.3.2   High Speed Train

Air resistance, roll resistance, slope resistance, acceleration resistance, and rail curvature resistance are a few of the drags that the train experiences. However, the computation of acceleration resistance is required for local and intercity trains since they stop more frequently. The acceleration force is proportional to the train mass and acceleration.

The force preventing motion when a body rolls on a surface is known as the rolling resistance R_R (Wikipedia 2023e). On a train, this is depicted by the contact between rail and the train wheel which can be calculated by multiplying the weight of the train and the rolling resistance coefficient μ_R. To calculate the rolling resistance of a high speed train, (3.30) of the car can be used. The rolling resistance for railroad wheel or rail is assumed around 0.0015 (Scholz 2022b).

The train's aerodynamic drag is similar to car's aerodynamic resistance in (3.29), which is proportional to square of train speed. c_d is the aerodynamic drag coefficient and it may vary for every type or train. It refers to the train's nose shape.

There are still a number of more train drag types. Figure 3.6 can display the total drag at each cruise speed to summarize the entire drag of a train, particularly a high-speed train.
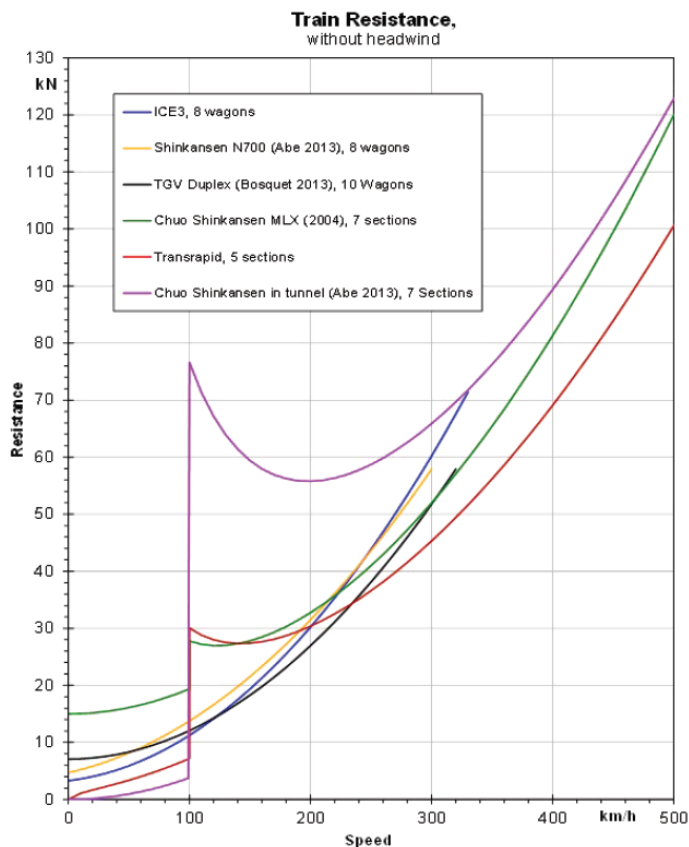
Figure 3.6 Resistances of high speed train (Fritz 2018)

By selecting the cruise speed shown in Figure 3.6, the train resistance will be determined at that speed, and (3.32) can be used to determine the lift-to-drag ratio of the train. The noteworthy aspect of this phenomenon is the significant resistance exhibited by the Chuo Shinkansen at a velocity of 100 km/h, which can be attributed to the considerable magnetic resistance of an EDS (electro-dynamic system) during the initial stages of levitation. It is

worth noting that the system remains supported by wheels until approximately 100 km/h (Fritz 2018).

The sample that been used in this paper are ICE 3 and TGV Duplex, which are electrically powered. And the data from Scholz (2021) represents the average energy consumption of the train. The focus of examination pertains to the energy expended by a train that maintains a consistent speed from its starting point to its final destination. However, conducting such an analysis under the identical conditions is not feasible. Therefore, the energy source provided by Scholz (2021) is utilized for this purpose. Then to calculate the primary energy it should be multiplied with primary energy factor k_{PEF} 2.1 (Scholz 2019).

$$\frac{E_{prim}}{s \cdot m_{pl}} = k_{PEF} \cdot \frac{E}{s \cdot m_{pl}} \tag{3.33}$$

3.3.3   Human and Animal

The other way to transport passenger is by the human itself, either on feet or by bicycle, or with the help of animal, such as horse. The weight and speed are divided by the power required for them to move in order to determine the lift-to-drag ratio of humans and animals. It can be divided into three categories for humans: walking, marching fast, and running. Cycling for people on bicycles can be divided into three categories: pleasure trip, speeding on highway, or at the racetrack. Also, it can be classified for horses depending on whether they are trotting, walking quickly, or active as racing horses.

$$\frac{L}{D} = \frac{m \cdot V}{P} \tag{3.34}$$

The value of energy per payload and range required from humans to walk, run and ride a bicycle can be found from Wikipedia (2023f). Ebert (2020) provides information on energy expenditure for horses. The energy value employed in this study is the mean energy value across all categories.

3.4   Pipeline Transport

3.4.1   Hyperloop

One type of pipeline transportation that moves people is the hyperloop. The idea is to travel with 28 passengers or even with cars under the speed of sound. They may glide with little

resistance on air cushions made from air that a compressor has sucked out in front of the vehicles. Elon Musk proposed the concept in a white paper in August 2013, stating that it would enable people to travel distances of up to 1200 kilometres far more quickly and sustainably than by air while also being much more affordable than by rail. Its financial and technological presumptions were questioned soon after publication. Following multiple unmanned test flights, a test run including humans was conducted for the first time on November 8, 2020, in Las Vegas, with the capsule traveling through a 500 m test tube at a speed of 172 km/h. At full occupancy with 840 passengers, SpaceX forecasted an energy consumption of 4.4 kWh/100 km per person for the Los Angeles to San Francisco route in 2013 by Hyperloop Alpha (Wikipedia 2023g). The utilization of solar panels leads to the assumption that the primary energy source aligns with the energy consumption.
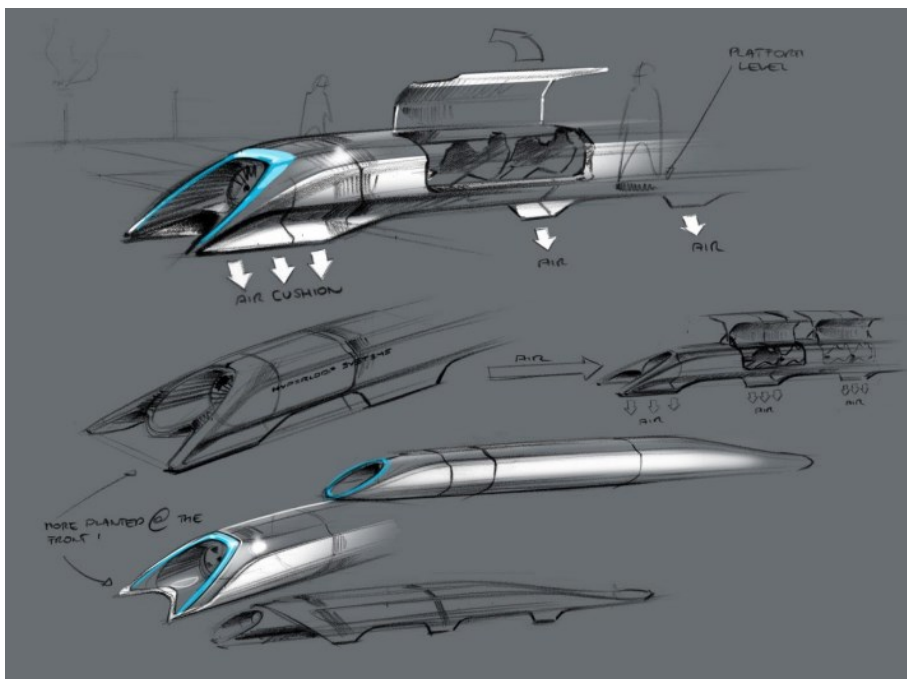
Figure 3.7   Hyperloop passenger transport capsule conceptual design sketch (Musk 2013)

Aerodynamic drag is one of the drag in the hyperloop as for high-speed vehicles, aerodynamic drag increases proportionally to the cube of speed, and the hyperloop capsule glides through air cushions. Additionally, the weight of the capsules is supported by air bearings that use a compressed air reservoir to operate. This is because air bearings have less friction, especially for high-speed vehicles, compared to other interfaces like rail tracks, which create friction drag. Air bearings also have drag, but it is very minimal and they are also inexpensive at cost (Musk 2013). So the lift to drag ratio of hyperloop can be calculated as,

$$\frac{L}{D} = \frac{m \cdot g}{R_A + R_B} \tag{3.35}$$

The lift-to-drag ratio can be calculated by multiplying the lift-to-drag by the ratio of payload to total mass.

3.4.2 Oil and Gas Pipeline

Oil and gas can also be transported by pipeline in addition to tanker transport. Pipelines are used to carry crude oil within continents, whilst tankers are used to transfer it between continents (Wagner 2017). Pump stations along the pipes move the oil and gas through the pipelines. The pressure differential Δp could be utilized to compute the lift-to-drag ratio (Herz 2004).

$$\Delta p = \frac{1}{2} \cdot \rho \cdot V^2 \cdot \lambda \cdot \frac{l}{d} \tag{3.36}$$

λ is the pipe friction coefficient and the Blasius correlation is a widely used formula for approximating the calculation of the smooth tube's pressure loss behaviour in Reynolds number smaller than 10^{-5} (Herz 2004).

$$\lambda = \frac{0.3164}{\sqrt[4]{Re}} \tag{3.37}$$

To determine the Reynolds number, use the following formula:

$$Re = \frac{V \cdot d}{\nu} \tag{3.38}$$

d is the diameter of the pipe and ν is the kinematic viscosity of the substance. If the given value is dynamic viscosity μ, then it should be converted to kinematic viscosity with the input of density ρ using the following formula:

$$\nu = \frac{\mu}{\rho} \tag{3.39}$$

In order to offer a correlation to the lift-to-drag ratio, the following formula[2] were constructed in relation of pressure difference formula in (3.36), power, volume flow rate and mass flow rate:

$$\frac{L}{D} = \frac{m \cdot g}{\Delta p \cdot A} = \frac{2 \cdot d \cdot g}{\lambda \cdot v^2} \tag{3.40}$$

In order to determine the lift-to-drag ratio pertaining to the payload of an oil and gas pipeline, it should be noted that the value is equivalent to the lift-to-drag ratio, given that the payload is the only entity in motion and no vehicle is in transportation. In the context of a pipeline system powered by diesel-operated pumps and utilizing 10% of its payload for operational

---

[2]   The equation refers to Prof. Scholz's explanation during thesis supervision, sent through his email.

purposes (Göß 2017), it can be observed that the lift-to-drag ratio is subject to a multiplication factor of 0.9.

Then the pressure difference formula in (3.36), power, volume flow rate and mass flow rate and also with the addition of energy formula are established further to discover the energy consumption per payload and range of the pipeline[3].

$$\frac{E}{s \cdot m_{pl}} = \frac{1}{2} \cdot V^2 \cdot \frac{\lambda}{d} \tag{3.41}$$

In order to generate the necessary pressure, it is imperative to utilize pumps or compressors. The level of efficiency is approximately 0.75 (Kollmar 2023). When the pump is powered by the gas or fuel from the pipeline, with an efficiency of 0.3, the consumption rate is increased by a factor of 4.4, as calculated by dividing 1 by the product of 0.3 and 0.75. It is noteworthy that, as per Göß (2017), a proportion of 10% of the oil or gas being transported is allocated for operational purposes. Consequently, the mass of the payload being transported is only 90%, leading to a division of the energy consumption per unit of payload and mass by 0.9.

$$\left(\frac{E}{s \cdot m_{pl}}\right)_{diesel/gas} = \frac{E}{s \cdot m_{pl}} \cdot \frac{1}{0.75 \cdot 0.3 \cdot 0.9} \tag{3.42}$$

And the efficiency of the pump, when it is powered electrically, is 0.9.

$$\left(\frac{E}{s \cdot m_{pl}}\right)_{electric} = \frac{E}{s \cdot m_{pl}} \cdot \frac{1}{0.75 \cdot 0.9} \tag{3.43}$$

To calculate primary energy, electrically powered pumps are multiplied by a factor of 2.1 and diesel or gas operated pumps are multiplied by a factor of 1.1. (Scholz 2019)

According to Banks (1977), neither technological additions nor technological advances in oil and gas pipelines will occur significantly in the US due to the decline in oil and gas production in the US. However, the reach will be extended, new pipelines will be used because imports must be implemented.

---

[3] The equation refers to Prof. Scholz's explanation during thesis supervision, sent through his email.

4 Parameters for the Modes of Transportation

4.1 Air Transport

4.1.1 Subsonic Fixed-Wing Aircraft

Table 4.1 presents a range of parameters that can be utilized to determine the maximum lift-to-drag ratio of fixed-wing aircraft. (3.2) will be used to calculate an aircraft's maximum lift-to-drag ratio or minimum drag. The ratio of wetted area and wing area for typical passenger jets can be seen in Figure 3.2.

The parameter k_E through range classification according to (Scholz 2022a) and aspect ratio A through (3.3) for several aircraft.

Table 4.1 The required parameters of subsonic fixed-wing aircraft to calculate maximum lift-to-drag ratio (Scholz 2022a) (Jenkinson 2001)

Aircraft	S_{wet}/S_W	Range	k_E	A
Airbus				
A321-200	7.01	Medium Range	16.19	9.39
A320-200	6.35	Medium Range	16.19	9.39
A300-600R	5.95	Medium Range	16.19	7.73
A310-300	5.97	Medium Range	16.19	8.80
A340-300	5.51	Long Range	17.25	9.26
Boeing				
B747-400	6.30	Long Range	17.25	7.39
B757-200	5.61	Medium Range	16.19	7.82
B737-300	5.96	Medium Range	16.19	9.17
B767-300	5.44	Long Range	17.25	7.99
McDonell Douglas				
MD90-30	6.56	Short Range	15.15	9.62
MD-11	5.56	Long Range	17.25	7.91
Fokker				
Fokker 100	6.26	Short Range	15.15	8.43
Tupolev				
TU-154M	5.07	Short Range	15.15	7.00
Northop				
YB-49	2.20	Long Range	17.25	7.39
Avro Vulcan				
Avro Vulcan	2.90	Long Range	17.25	2.78
Cargo Aircraft				
B747-400	6.30	Long Range	17.25	7.39
MD-11	5.56	Long Range	17.25	7.91

The maximum lift-to-drag ratio in Table 4.2 can be calculated using (3.2) with the value of S_{wet}/S_W, k_E and aspect ratio A from Table 4.1. (3.1) will be applied to determine the lift-to-drag ratio based on the payload mass in Table 4.3. The total mass specially for aircraft is the maximum take-off mass m_{MTO}, which then based on (3.1) can be written as,

$$\left(\frac{L}{D}\right)_{pl} = \frac{m_{pl}}{m_{MTO}} \cdot \frac{L}{D}$$

(4.1)

Table 4.2   The maximum L/D ratio and cruising speed of subsonic fixed-wing aircraft (Jenkinson 2001)

Aircraft	$\left(\dfrac{L}{D}\right)_{max}$	V m/s
Airbus		
A321-200	18.74	231.48
A320-200	19.69	230.45
A300-600R	18.46	246.91
A310-300	19.65	248.97
A340-300	22.37	257.20
Boeing		
B747-400	18.69	252.58
B757-200	19.11	263.89
B737-300	20.09	252.57
B767-300	20.90	251.03
McDonell Douglas		
MD90-30	18.35	224.79
MD-11	20.57	262.42
Fokker		
Fokker 100	17.58	212.96
Tupolev		
TU-154M	17.80	236.11
Northop		
YB-49	31.61	191.78
Avro Vulcan		
Avro Vulcan	16.89	253.60
Cargo Aircraft		
B747-400	18.69	252.58
MD-11	20.57	262.42

Table 4.3   The lift-to-drag ratio regarding payload of subsonic fixed-wing aircraft (Jenkinson 2001)

Aircraft	m_{mpl} kg	m_{MTO} kg	m_{pl}/m_{MTO} %	$\left(\dfrac{L}{D}\right)_{max,pl}$
Airbus				
A321-200	25300	89000	28.43	5.33
A320-200	16200	73500	22.04	4.34
A300-600R	41100	170500	24.11	4.45
A310-300	33300	150000	22.20	4.36
A340-300	48150	271000	17.77	3.97
Boeing				
B747-400	61186	396830	15.42	2.88
B757-200	25690	115900	22.17	4.24
B737-300	16030	56470	28.39	5.70
B767-300	39140	156489	25.01	5.23
McDonell Douglas				
MD90-30	17350	70760	24.52	4.50
MD-11	55566	283720	19.58	4.03
Fokker				
Fokker 100	11108	43090	25.78	4.53
Tupolev				
TU-154M	18000	100000	18.00	3.20
Northop				
YB-49	4536	87969	5.16	1.63
Avro Vulcan				
Avro Vulcan	10000	77111	12.97	2.19
Cargo Aircraft				
B747-400	113000	396830	28.48	5.32
MD-11	91962	283720	32.41	6.67

In Table 4.4, he specific air range (SAR) can be calculated using (3.4) with the data of specific fuel consumption from Hammami (2021a) or calculation of SFC in cruise with (3.5). The energy consumption per payload and range could then be calculated using (3.7) by multiplying the 43 MJ/kg heating value of kerosene. Multiplying the energy consumption per payload range at the end by a factor of 1.1 in (3.8) yielded the primary energy consumption per payload and range (Scholz 2019).

Table 4.4   The primary energy consumption per distance and payload of subsonic fixed-wing aircraft (Hammami 2021a)

Aircraft	SFC_{Cruise} Kg/Ns	SAR m/kg	m_f/s kg/m	$E/(s \cdot m_{pl})$ J/mkg	$E_{prim}/(s \cdot m_{pl})$ J/mkg
Airbus					
A321-200	$1.60 \cdot 10^{-5}$	310.22	0.0032	5.48	6.03
A320-200	$1.53 \cdot 10^{-5}$	410.96	0.0024	6.46	7.10
A300-600R	$1.63 \cdot 10^{-5}$	167.17	0.0060	6.26	6.88
A310-300	$1.62 \cdot 10^{-5}$	204.71	0.0049	6.31	6.94
A340-300	$1.53 \cdot 10^{-5}$	141.30	0.0071	6.32	6.95
Boeing					
B747-400	$1.63 \cdot 10^{-5}$	74.39	0.0134	9.45	10.39
B757-200	$1.82 \cdot 10^{-5}$	244.32	0.0041	6.85	7.54
B737-300	$1.87 \cdot 10^{-5}$	488.60	0.0020	5.49	6.04
B767-300	$1.60 \cdot 10^{-5}$	213.39	0.0047	5.15	5.66
McDonell Douglas					
MD90-30	$9.83 \cdot 10^{-6}$	604.17	0.0017	4.10	4.51
MD-11	$1.58 \cdot 10^{-5}$	122.39	0.0082	6.32	6.96
Fokker					
Fokker 100	$1.93 \cdot 10^{-5}$	456.87	0.0022	8.47	9.32
Tupolev					
TU-154M	$2.19 \cdot 10^{-5}$	195.21	0.0051	12.24	13.46
Northop					
YB-49	$2.84 \cdot 10^{-5}$	247.38	0.0040	38.32	42.15
Avro Vulcan					
Avro Vulcan	$2.54 \cdot 10^{-5}$	223.37	0.0045	19.25	21.18
Cargo Aircraft					
B747-400	$1.62 \cdot 10^{-5}$	74.39	0.0134	5.12	5.63
MD-11	$1.58 \cdot 10^{-5}$	112.39	0.0082	3.82	4.20

4.1.2   Supersonic Fixed-Wing Aircraft

The cruise speed of Concorde is 599 m/s. To convert speed to Mach number, depending on (3.10), it is necessary to know the speed of sound at Concorde's cruising altitude. At an altitude of 60000 ft or 18300 m, the speed of sound is 573.8 kt or 295.2 m/s.

$$M = \frac{599.44 \text{ m/s}}{295.2 \text{ m/s}} = 2.03 \tag{4.2}$$

The maximum lift-to-drag ratio can therefore be obtained as follows:

$$\left(\frac{L}{D}\right)_{max} = \frac{3(2.03 + 3)}{2.03} = 7.432 \tag{4.3}$$

To calculate the lift-to-drag ratio regarding payload mass, the ratio of payload mass m_{pl} to maximum take-off mass m_{MTO} needs to be multiplied by the maximum lift-to-drag.

$$\left(\frac{L}{D}\right)_{max,pl} = 7.432 \cdot \frac{13380 \text{ kg}}{185000 \text{ kg}} = 0.538 \tag{4.4}$$

The energy consumption of Concorde per payload and range, calculated using the principle of specific air range (SAR) as in subsonic fixed-wing aircraft, is 43.78 J/mkg, whereas its primary energy consumption is 48.16 J/mkg.

4.1.3   Rotorcraft

The R44 Raven I and II, AS350 B3, and EC120 B are examples of rotorcraft powered vehicles that will be explained. The computation of the lift-to-drag ratio of helicopters shall be conducted based on three distinct parameters, namely the maximum take-off weight m_{MTO}, continuous power P_{cont}, and cruising speed V in Table 4.5.

Table 4.5   The lift-to-drag ratio of helicopter (Robinson 2022) (Eurocopter 2009) (Eurocopter 2007)

Helicopter	m_{MTO} kg	P_{cont} kW	V m/s	L/D
R44 Raven I	1089	153.75	55.56	3.86
R44 Raven II	1134	153.75	56.11	4.06
AS350 B3	2250	543	65.28	2.65
EC120 B	1715	335	56.67	2.85

As applied to other aircraft types, the lift-to-drag ratio will be calculated in Table 4.6 by dividing the payload mass and maximum take-off mass. The energy consumption per payload and range can be calculated in Table 4.7 by dividing the fuel mass m_f by the range s and payload mass m_{pl}, which will then be multiplied by a factor of 1.1 to get the primary energy consumption per payload and range because the helicopter operates using kerosene.

Table 4.6   The lift-to-drag ratio regarding payload mass of helicopter (Robinson 2022) (Eurocopter 2009) (Eurocopter 2007)

Helicopter	m_{pl} kg	m_{pl}/m_{MTO} %	$\left(\frac{L}{D}\right)_{pl}$
R44 Raven I	351	32.23	1.24
R44 Raven II	371	32.72	1.33
AS350 B3	1009	44.84	1.19
EC120 B	725	42.27	1.20

Table 4.7 Primary energy consumption per payload and range of helicopter (Robinson 2022) (Eurocopter 2009) (Eurocopter 2007)

Helicopter	m_f kg	s m	$m_f/(s \cdot m_{pl})$ kg/mkg	$E/(s \cdot m_{pl})$ J/mkg	$E_{prim}/(s \cdot m_{pl})$ J/mkg
R44 Raven I	80	550000	$4.144 \cdot 10^{-7}$	17.82	19.60
R44 Raven II	80	550000	$3.920 \cdot 10^{-7}$	16.86	18.54
AS350 B3	426	657000	$6.426 \cdot 10^{-7}$	27.63	30.40
EC120 B	321	710000	$6.236 \cdot 10^{-7}$	26.81	29.50

4.1.4 Airship

The coefficient of drag c_{DV} and arbitrary reference area S_V of LZ129 must first be determined before the drag D_0 Hindenburg can be estimated as to be seen in Table 4.8.

Table 4.8 Zero lift drag coefficient of Hindenburg (Grossman 2017a) (Grossman 2017b) (Letadlanaplatne 2023)

Airship	l m	d m	d/l	V m/s	ν	Re	c_{DV}
LZ129 Hindenburg	245	41.20	0.17	34.72	$1.46 \cdot 10^{-5}$	582630136.99	0.012

And the arbitrary reference area from the volume of the airship can be calculated using (3.14) in Table 4.9.

Table 4.9 Wetted area of Hindenburg

Airship	V m³	S_V m²
LZ129 Hindenburg	200000	3419.95

The cruising altitude of LZ129 Hindenburg is 200 m and the cruising speed is 34.72 m/s (Grossman 2017). Then the air density according to international standard atmosphere at cruising altitude is 1.225 kg/m³. If these values are applied in (3.13), then

$$D_0 = \frac{1}{2} \cdot 1.225 \, \frac{\text{kg}}{\text{m}^3} \cdot \left(34.72 \, \frac{\text{m}}{\text{s}}\right)^2 \cdot 0.012 \cdot 3419.95 \, \text{m}^2 = 30551.54 \, \text{N} \qquad (4.5)$$

The airship's lift must be divided by the zero lift drag to obtain the lift-to-drag ratio. LZ129 Hindenburg can lift 232.000 kg (Engheim 2018).

$$\frac{L}{D} = \frac{232000 \, \text{kg} \cdot 9.81 \, \frac{\text{m}}{\text{s}^2}}{30551.54 \, \text{N}} = 74{,}49 \qquad (4.6)$$

The payload mass of Hindenburg is 9560 kg, which will results in ratio between payload mass and total mass of 4.12%. Then the lift to drag ratio with regards to payload mass can be calculated as,

$$\left(\frac{L}{D}\right)_{pl} = \frac{4.12}{100} \cdot 74.49 = 3.07$$

(4.7)

According to Grossman (2017), it used 130 kg/h of diesel fuel at normal cruising speed. To calculate the energy consumption per payload and range, the following equation according to fuel consumption from Grossman (2017), heating value of diesel, speed, and payload mass will be used.

$$\frac{E}{s \cdot m_{pl}} = \frac{130 \frac{kg}{h} \cdot H_L}{v \cdot m_{pl}} = \frac{130 \frac{kg}{h} \cdot 43 \text{ MJ}}{34.72 \frac{m}{s} \cdot 9560 \text{ kg}} = 4.68 \frac{J}{mkg}$$

(4.8)

LZ129 Hindenburg is powered with diesel, so to get the primary energy consumption per payload and range, (4.8) should be multiplied with 1.1.

$$\frac{E_{prim}}{s \cdot m_{pl}} = 1.1 \cdot 4.68 \frac{J}{mkg} = 5.15 \frac{J}{mkg}$$

(4.9)

4.1.5 Glider

This paper will utilize the Grob 103 and ASW 28 glider models. Table 4.10 provides a means of calculating the lift-to-drag ratio in relation to payload mass. This involves multiplying the lift-to-drag ratio value by the ratio of payload mass to the maximum take-off mass of the glider.

Table 4.10 The lift-to-drag ratio and the lift-to-drag ratio regarding payload mass of glider (Utah Soarding Association 2019) (AS 2023)

Glider	v_{Cr} m/s	L/D	m_{pl}/m_{MTO} %	$\left(\frac{L}{D}\right)_{pl}$
Grob 103	30.85	36	32.11	11.56
ASW 28	55.56	45	24.76	11.14

The Glider's operation does not necessitate the use of fuel, resulting in a consumption of zero fuel or energy per payload and range.

4.2   Water Transport

4.2.1   Bulker, Tanker and Container Vessel

The Excel calculation tool from Kristensen (2017b) will be used for predicting drag and energy demand from ships using empirical and semi-empirical methods based only ship type and bulk parameters. The dead weight tonnage DWT should be inputted to the Excel table from Kristensen (2017b). Subsequently, additional particulars pertaining to the vessel's classification, including but not limited to its displacement, length between perpendiculars, draught, and wetted surface area, shall be exhibited. As a result, the total resistance denoted as R_T shall be ascertained and the values from each vessel type are listed in Table 4.11. These results applied at water temperature of 15 °C.

Table 4.11   Total resistance of bulker, tanker and container vessel (Kristensen 2017b)

Vessel	DWT tons	R_T kN
Bulker		
Small Bulker	7000	186
Handysize Bulker	20000	351
Handymax Bulker	45000	682
Panamax Bulker	75000	716
Capesize	100000	880
VLBC	250000	1384
Tanker		
Small Tanker	7000	228
Handysize Tanker	20000	398
Handymax Tanker	45000	697
Panamax Tanker	60000	856
Aframax	100000	888
Suezmax	150000	1057
VLCC	250000	1826
Container Vessel		
Feeder Container Vessel	32832	1137
Panamax (typ.2) Container Vessel	45320	1480
Post Panamax (typ.3) Container Vessel	63797	1842
Post Panamax (typ.4) Container Vessel	163800	3449

The loaded displacement Δ contains the weight of the vessel itself plus cargo and fuel. The lift-to-drag ratio is determined with (3.24) in Table 4.12. The ratio of payload mass to total weight is calculated similarly to how an airplane is calculated. But the maximum tonnage displacement Δ is employed rather than the maximum weight and take-off weight m_{MTO}. And the payload mass to maximum tonnage displacement could be used to calculate the lift-to-drag ratio regarding to payload mass $\left(\frac{L}{D}\right)_{pl}$ in Table 4.13.

$$\left(\frac{L}{D}\right)_{pl} = \frac{m_{pl}}{\Delta} \cdot \frac{L}{D} \qquad (4.10)$$

Table 4.12 The maximum lift-to-drag ratio and cruising speed of bulker, tanker and container vessel (Kristensen 2017b)

Vessel	Δ tons	L/D	V m/s
Bulker			
Small Bulker	9259	488.34	6.78
Handysize Bulker	25543	713.89	7.10
Handymax Bulker	53752	773.18	7.36
Panamax Bulker	86189	1180.89	7.51
Capesize	115435	1286.84	7.61
VLBC	280222	1986.26	7.71
Tanker			
Small Tanker	9599	413.01	7.14
Handysize Tanker	25911	638.66	7.47
Handymax Tanker	54798	771.26	7.71
Panamax Tanker	71749	822.26	7.71
Aframax	117183	1294.56	7.71
Suezmax	173841	1613.42	7.71
VLCC	285967	1536.33	7.97
Container Vessel			
Feeder Container Vessel	43564	375.87	10.28
Panamax (typ.2) Container Vessel	60330	399.89	10.74
Post Panamax (typ.3) Container Vessel	83620	445.34	11.26
Post Panamax (typ.4) Container Vessel	212140	603.39	12.08

Table 4.13 The lift-to-drag ratio regarding payload of bulker, tanker and container vessel (Kristensen 2017b)

Vessel	m_{pl} ton	m_{pl}/Δ %	$\left(\frac{L}{D}\right)_{pl}$
Bulker			
Small Bulker	5670	61.24	299.05
Handysize Bulker	17100	66.95	477.92
Handymax Bulker	38475	71.58	553.43
Panamax Bulker	64125	74.40	878.58
Capesize	85500	74.07	953.13
VLBC	213750	76.28	1515.09
Tanker			
Small Tanker	5670	59.07	243.96
Handysize Tanker	17100	66.00	412.48
Handymax Tanker	38475	70.21	541.52
Panamax Tanker	51300	71.50	587.91
Aframax	85500	72.96	944.54
Suezmax	128250	73.77	1190.29
VLCC	213750	74.75	1148.35
Container Vessel			
Feeder Container Vessel	22408	51.44	193.34
Panamax (typ.2) Container Vessel	31702	52.55	210.13
Post Panamax (typ.3) Container Vessel	46253	55.31	246.33
Post Panamax (typ.4) Container Vessel	146601	69.11	416.98

It is necessary to multiply the energy demand per payload and range by factor 1.1 in order to determine the primary energy consumption per payload and range (Scholz 2019) as seen in Table 4.14.

Table 4.14 Primary energy consumption per payload and range for bulker, tanker and container vessel (Kristensen 2017b)

Vessel	$E/(s \cdot m_{pl})$ J/mkg	$E_{prim}/(s \cdot m_{pl})$ J/mkg
Bulker		
Small Bulker	0.140	0.154
Handysize Bulker	0.082	0.090
Handymax Bulker	0.056	0.062
Panamax Bulker	0.040	0.044
Capesize	0.038	0.042
VLBC	0.023	0.025
Tanker		
Small Tanker	0.167	0.184
Handysize Tanker	0.092	0.101
Handymax Tanker	0.063	0.069
Panamax Tanker	0.050	0.055
Aframax	0.039	0.043
Suezmax	0.030	0.033
VLCC	0.025	0.028
Container Vessel		
Feeder Container Vessel	0.154	0.169
Panamax (typ.2) Container Vessel	0.131	0.144
Post Panamax (typ.3) Container Vessel	0.113	0.124
Post Panamax (typ.4) Container Vessel	0.067	0.074

4.2.2 Cruise Ship

(3.22) will be applied to determine the cruise ship's wetted surface area in Table 4.15. It will be necessary to know the values of the ship's draught T, also known as draft, volume displacement of the ship ∇, and length between perpendicular L_{pp}.

Table 4.15 The wetted area of the cruise ships (Academic 2023) (Wikipedia 2023h) (Ships Hub 2019) (Ship Technology 2015)

Ship	T m	Δ kg	∇ m^3	L_{pp} m	S_W m^2
Queen Mary 2	10.3	79287·10^3	77732.35	301	13137.77
Norwegian Spirit	7.92	75388·10^3	73909.80	235.6	12816.77
P&O Britania	8.3	141000·10^3	138235.29	306	21496.83

(3.19) can be used to get the cruise ship's coefficient of friction C_F. Before anything further, though, the Reynolds number needs to be calculated using (3.20) and a kinematic water viscosity ν of $1.004 \cdot 10^{-6}$.

The value of the coefficient of friction can then be used as the total resistance coefficient C_T in (3.18) to compute the total resistance R_T in Table 4.16.

The lift to drag ratio was then calculated using (3.24) by dividing the ship's loaded displacement and gravity acceleration $\Delta \cdot g$ with the total resistance R_T.

Table 4.16   The lift-to-drag ratio of cruise ships (Academic 2023) (Wikipedia 2023h) (Ships Hub 2019) (Ship Technology 2015)

Ship	V m/s	Re	C_F	R_T N	L/D
Queen Mary 2	13.38	$3.60 \cdot 10^9$	0.00131	$1.57 \cdot 10^6$	494.06
Norwegian Spirit	10.80	$2.28 \cdot 10^9$	0.00139	$1.06 \cdot 10^6$	699.75
P&O Britania	11.31	$3.10 \cdot 10^9$	0.00134	$1.88 \cdot 10^6$	737.12

The calculation of the lift-to-drag ratio regarding to the payload mass is performed in a manner analogous to that which is performed for bulkers and tankers which then be presented in Table 4.17. For cruise ship, the payload mass will be assumed as the weight of the passengers and crews, which is in Chapter 3.2.2 already defined with 88 kg, with their possible luggage around 22 kg.

Table 4.17   The lift-to-drag ratio regarding payload of cruise ship (Academic 2023) (Wikipedia 2023h) (Ships Hub 2019) (Ship Technology 2015)

Ship	Passenger and crew pax	m_{pl} kg	m_{pl}/Δ %	$\left(\frac{L}{D}\right)_{pl}$
Queen Mary 2	3948	434280	0.55	2.71
Norwegian Spirit	2930	322300	0.43	2.99
P&O Britania	5530	608300	0.43	3.18

The energy consumption per payload range can therefore be calculated by multiplying the fuel consumption of passenger ships by the heating value of diesel and divided by the payload. At the end, the primary energy can be calculated by multiplying the energy consumption per payload range with the factor 1.1 as to be seen in Table 4.18.

Table 4.18   The primary energy consumption of cruising ships (Academic 2023) (Wikipedia 2023h) (Ships Hub 2019) (Ship Technology 2015)

Ship	m_f/s kg/m	l/m	E/s J/m	$E/(s \cdot m_{pl})$ J/mkg	$E_{prim}/(s \cdot m_{pl})$ J/mkg
Queen Mary 2	0.12		5293457	12.19	13.41
Norwegian Spirit		0.11	3777019	11.72	12.89
P&O Britania		0.26	9177649	15.09	16.60

4.3   Land Transport

4.3.1   Car, Truck and Bus

The total drag of the vehicle consists of aerodynamic drag R_A and rolling resistance R_R. The rolling resistance can be calculated using (3.30) in Table 4.19 with rolling friction coefficient μ_R in Table 3.3. The track was categorized in asphalt, which was normally used in the city, and also in earth way. The mass defined by the curb weight m_{Curb} and the maximal payload, which indicated by the maximum passenger capacity. Each passenger's weight was considered to be 88 kg, as described in Chapter 3.1.2.

Table 4.19   The rolling resistance of car, truck and bus (Kmet 2022) (Carexpert 2023) (Wikipedia 2023i) (Shacman 2020) (Scania 2023) (Mercedes-Benz 2023)

Vehicle	m_{Curb} kg	m_{pl} kg	μ_R	m kg	R_R N
Car					
Mercedes G-Class (City)	2460	440	0.015	2900	426.74
Toyota Prius (City)	1365	440	0.015	1805.31	265.65
Tesla 3 (City)	1700	440	0.015	2140	314.90
Audi E-tron (City)	2500	440	0.015	2940	432.62
Mercedes G-Class (Earth way)	2460	440	0.05	2900	1422.45
Toyota Prius (Earth way)	1365	440	0.05	1805.31	885.51
Tesla 3 (Earth way)	1700	440	0.05	2140	1049.67
Audi E-tron (Earth way)	2500	440	0.05	2940	1442.07
Truck					
Scania P380 (City)	14000	27000	0.015	41000	6033.15
Shacman (City)	14600	16400	0.015	31000	4561.61
Scania P380 (Earthway)	14000	27000	0.05	41000	20110.50
Shacman (Earthway)	14600	16400	0.05	31000	15205.50
Bus					
Tourisimo L (City)	13400	6500	0.015	19900	2928.29
Tourisimo L (Earthway)	13400	6500	0.05	19900	9760.95

The aerodynamic drag can be calculated using (3.29) in Table 4.20 with the specification of coefficient of drag c_d, frontal area A_f of the car and square of its cruising speed V^2. The assumption of air density is 1.225 kg/m³.

After that, the total drag R_T as well as the lift-to-drag ratio can be determined as in (3.31) and (3.32). The lift-to-drag ratio regarding to payload mass in Table 4.21 can be calculated by multiplying the ratio of payload mass total mass with the lift-to-drag ratio.

Table 4.20 The aerodynamic drag of car, truck and bus (Kmet 2022) (Ecomodder 2018) (Shacman 2020) (Scania 2023) (Mercedes-Benz 2023)

Vehicle	c_d	A_f m²	V m/s	R_A N
Car				
Mercedes G-Class (City)	0.53	2.97	27.78	744.05
Toyota Prius (City)	0.25	2.20	27.78	259.57
Tesla 3 (City)	0.23	2.22	27.78	241.35
Audi E-tron (City)	0.28	2.65	27.78	350.73
Mercedes G-Class (Earth way)	0.53	2.97	16.67	267.92
Toyota Prius (Earth way)	0.25	2.20	16.67	93.47
Tesla 3 (Earth way)	0.23	2.22	16.67	86.91
Audi E-tron (Earth way)	0.28	2.65	16.67	126.29
Truck				
Scania P380 (City)	0.90	9.63	27.78	4094.62
Shacman (City)	0.75	8.59	27.78	3045.44
Scania P380 (Earthway)	0.90	9.63	16.67	1474.42
Shacman (Earthway)	0.75	8.59	16.67	1096.62
Bus				
Tourisimo L (City)	0.33	9.38	27.78	1463.77
Tourisimo L (Earthway)	0.33	9.38	16.67	527.08

Table 4.21 The lift-to-drag ratio and the lift-to-drag ratio regarding payload for car, truck and bus

Vehicle	R_T N	L/D	m_{pl}/m %	$\left(\frac{L}{D}\right)_{pl}$
Car				
Mercedes G-Class (City)	1170.79	24.30	15.17	3.69
Toyota Prius (City)	525.22	33.72	24.37	8.22
Tesla 3 (City)	556.24	37.74	20.56	7.76
Audi E-tron (City)	783.35	36.82	14.97	5.51
Mercedes G-Class (Earth way)	1690.37	16.83	15.17	2.55
Toyota Prius (Earth way)	978.97	18.09	24.37	4.41
Tesla 3 (Earth way)	1136.58	18.47	20.56	3.80
Audi E-tron (Earth way)	1586.36	18.39	14.97	2.75
Truck				
Scania P380 (City)	10127.77	39.71	65.85	26.15
Shacman (City)	7607.09	39.98	52.90	21.15
Scania P380 (Earthway)	21584.92	18.63	65.85	12.27
Shacman (Earthway)	16302.12	18.65	52.90	9.87
Bus				
Tourisimo L (City)	4392.05	44.45	32.66	14.52
Tourisimo L (Earthway)	10288.03	18.98	32.66	6.20

The determination of fuel efficiency per payload range can be conducted independently for gasoline-powered vehicles and electric vehicles. For gasoline-powered vehicles, this can be achieved by dividing the fuel consumption by the weight of the payload. The calculation of primary energy consumption per payload range for a gasoline fuel vehicle involves the multiplication of the energy consumption per payload range by a factor of 1.1. In the context of electric vehicles, it is necessary to apply a multiplication factor of 2.1 to the energy

consumption per payload range (Scholz 2019). The values of primary energy consumption per payload and range are presented in Table 4.22.

Table 4.22 The primary energy consumption per payload range for cars (EV Database 2021) (EV Database 2022) (Oak Ridge Laboratory 2023a) (Oak Ridge Laboratory 2023b) (Webfleet 2020) (Mercedes-Benz 2019)

Vehicle	s/E m/J	E/s J/m	$E/(s \cdot m_{pl})$ J/mkg	$E_{prim}/(s \cdot m_{pl})$ J/mkg
Car				
Mercedes G-Class	0.000186		12.21	13.43
Toyota Prius	0.000692		3.29	3.61
Tesla 3		543.6	1.24	2.59
Audi E-tron		853.2	1.94	4.07
Truck				
Scania P380			0.47	0.52
Shacman			0.55	0.61
Bus				
Tourisimo L			1.11	2.34

4.3.2 High Speed Train

During a train's travel, total drag is the sum of rolling resistance and aerodynamic resistance. Using (3.29) and (3.30), the aerodynamic drag and rolling resistance may be determined.

However, the acceleration of the large passenger train is equally crucial because it stops at multiple stations. Due to the complexity of determining acceleration, the data of total resistance from Chapter 3.3.2 in Figure 3.6 should be used for the calculation of lift-to-drag ratio in Table 4.23, which includes aerodynamic drag, rolling resistance and acceleration resistance.

The service mass $m_{Service}$ is the net mass of a rail vehicle plus a fraction of the operating material supplies and people mass (Wikipedia 2023j).

Table 4.23 The lift-to-drag ratio of high speed train train (Wikipedia 2023k) (Wikipedia 2023l) (Fritz 2018)

Train	V km/h	m/s	$m_{Service}$ kg	R_T N	L/D
ICE 3	320	88.89	520040	70000	72.88
TGV Duplex	300	83.33	390000	52000	73.58

As indicated in Table 4.24, the lift-to-drag ratio regarding payload mass may be obtained through the multiplication of the lift-to-drag ratio by the ratio of payload mass and service mass.

Table 4.24 The lift-to-drag ratio of high speed train (Wikipedia 2023k) (Wikipedia 2023l) (Fritz 2018)

Train	Passenger pax	m_{pl} kg	$m_{pl}/m_{Service}$ %	$\left(\frac{L}{D}\right)_{pl}$
ICE 3	441	48819	9.39	6.84
TGV Duplex	508	56236	14.42	10.61

According to Scholz (2021), the trains' primary energy consumption is 60 Wh/pax km, which is equivalent to 1.95 J/mkg. The train derives its power output from electricity, resulting in a primary energy of 4.10 J/mkg.

4.3.3 Human and Animal

The power and mass parameters were sourced from Karman and Gabrielli's primary publication, as presented in Table 4.25. Following that, utilizing these parameters, the lift-to-drag ratio can be computed.

Table 4.25 The lift-to-drag ratio of human and animal (Gabrielli 1950)

Human and Animal	m kg	V m/s	P J/s	L/D
Human				
Human walking	70.29	1.34	62.64	14.76
Huan marching fast	61.22	4.02	223.71	10.80
100-yard runner	55.33	10.01	671.13	8.10
Bicycle				
Bicycle pleasure trip	83.90	6.93	186.43	30.59
Bicycle speeding on highway	72.56	11.18	350.48	22.70
Bicycle on racetrack	70.29	17.03	753.16	15.59
Horse				
Horse with carriage, fast step	1587.30	2.01	477.25	65.63
Horse with carriage, trotting	1201.81	4.02	633.85	74.83
Active racehorse	453.51	17.21	1491.40	51.34

As presented in Table 4.26, the lift-to-drag ratio with respect to payload mass can be calculated by multiplying the lift-to-drag ratio by the ratio of payload mass to total mass.

Given that the energy derives from the organism's metabolic processes, it follows that the primary energy consumption ought to be commensurate with the consumption of energy. Table 4.27 displays the values pertaining to energy consumption per payload and range for human and animal.

Table 4.26   The lift-to-drag ratio regarding payload of human and animal (Gabrielli 1950)

Human and Animal	m_{pl} kg	m_{pl}/m %	$\left(\frac{L}{D}\right)_{pl}$
Human			
Human walking	70.29	100	14.76
Huan marching fast	61.22	100	10.80
100-yard runner	55.33	100	8.10
Bicycle			
Bicycle pleasure trip	70.29	83.78	25.63
Bicycle speeding on highway	61.22	84.37	19.15
Bicycle on racetrack	55.33	78.71	12.27
Horse			
Horse with carriage, fast step	210.87	13.28	8.72
Horse with carriage, trotting	210.87	17.55	13.13
Active racehorse	55.33	12.20	6.26

Table 4.27   The primary energy consumption per payload and range of human and animal (Wikipedia 2023f) (Ebert 2020)

Human and Animal	$E/(s \cdot m_{pl})$ J/mkg	$E_{prim}/(s \cdot m_{pl})$ J/mkg
Human		
Human walking	2.00	2.00
Huan marching fast	2.00	2.00
100-yard runner	2.00	2.00
Bicycle		
Bicycle pleasure trip	1.10	1.10
Bicycle speeding on highway	1.10	1.10
Bicycle on racetrack	1.10	1.10
Horse		
Horse with carriage, fast step	4.05	4.05
Horse with carriage, trotting	4.05	4.05
Active racehorse	4.05	4.05

4.4   Pipeline Transport

4.4.1   Hyperloop

There are two variations of the Hyperloop Alpha, one for people and one for people and freight. From (3.35), the lift to drag ratio of the hyperloop alpha can be calculated as follows in Table 4.28,

Table 4.28   The lift-to-drag of Hyperloop Alpha (Musk 2013)

Hyperloop	V m/s	R_A N	R_B N	$m_{Service}$ kg	L/D
Hyperloop Alpha for passenger and cargo	339.75	910	187	26000	232.51
Hyperloop Alpha for passenger	339.75	310	140	15000	327.00

As presented in Table 4.29, the lift-to-drag ratio with respect to payload mass can be calculated by multiplying the lift-to-drag ratio by the ratio of payload mass to total mass.

Table 4.29 The lift-to-drag ratio regarding payload of hyperloop alpha (Musk 2013)

Hyperloop	m_{pl} kg	m_{pl}/m %	$\left(\frac{L}{D}\right)_{pl}$
Hyperloop Alpha for passenger and cargo	8900	34.23	79.59
Hyperloop Alpha for passenger	2800	18.67	61.04

As described in Chapter 3.4.1, their energy consumption per payload range is 4.4 kWh per passenger per 100 km, or 1.58 J/mkg. The main energy source is a solar panel with a primary energy factor of 1. So the primary energy consumption per payload and range of hyperloop alpha remains 1.58 J/mkg.

4.4.2 Oil and Gas Pipeline

The lift-to-drag ratio of oil and gas pipeline can be calculated in Table 4.30 using (3.40).

Table 4.30 The lift-to-drag ratio of oil and gas pipeline

Oil and gas pipeline	V m/s	d m	μ m²/s	Rn	λ	L/D
Water pipeline	2	1	0.00100	1994	0.047	103.59
Heavy oil pipeline	2	1	0.03000	66.67	0.111	44.30
Gas pipeline	10	1	0.00001	719424.46	0.011	18.06

The lift-to-drag ratio with regard to payload mass value is the same as the lift-to-drag ratio value since the pipe is fixed and does not move with the products being transported. But as in Chapter 3.4.2 explained, the diesel or gas pump needs to be multiplied with factor 0.9. Table 4.31 shows the results for both types of pump.

Table 4.31 Lift-to-drag ratio regarding payload mass of oil and gas pipeline

Oil and gas pipeline	$\left(\frac{L}{D}\right)_{pl,electric}$	$\left(\frac{L}{D}\right)_{pl,diesel/gas}$
Water pipeline	103.59	93.23
Heavy oil pipeline	44.30	39.87
Gas pipeline	18.06	16.25

The energy required for its operation according to (3.41) is listed in Table 4.32. The efficiency of pump or compressor for about 0.75 should be included.

Table 4.32 The energy consumption per payload range of oil and gas pipeline

Oil and gas pipeline	$E/(s \cdot m_{pl})$ J/mkg
Water pipeline	0.13
Heavy oil pipeline	0.30
Gas pipeline	0.72

The energy consumption per payload and range of gas pipeline, as presented in Table 4.32, exhibit a close resemblance to the transportation of natural gas from Siberian sources to Western Europe, spanning a distance of approximately 5000 km (Göß 2017). This transportation process involves injecting over 10% of the gas into the pipeline for operational purposes. Assuming a calorific value of 38 MJ/kg for natural gas, a 10% proportion is equivalent to 3.8 MJ/kg. Ultimately, the energy consumption is divided by the distance.

$$\frac{E}{s \cdot m_{pl}} = 3.8 \, \frac{MJ}{kg} \cdot \frac{1}{5000 \text{ km}} = 0.76 \, \frac{J}{mkg} \tag{4.11}$$

Some transportation pipelines are powered by diesel fuel and natural gas, while others rely on electric power as their source of propulsion. The values obtained from the two power sources are displayed in Table 4.33. (3.42) and (3.43) can be used as formula to calculate the energy in both types of pumps.

Table 4.33 The energy consumption per payload range of oil and gas pipeline powered by electric or diesel and gas

Oil and gas pipeline	$E/(s \cdot m_{pl})$ (electric) J/mkg	$E/(s \cdot m_{pl})$ (diesel/gas) J/mkg
Water pipeline	0.14	0.47
Heavy oil pipeline	0.33	1.09
Gas pipeline	0.80	2.68

Table 4.34 presents the primary energy per load and range values for oil and gas pipelines that are fuelled by either electricity or diesel/gas. A multiplication factor of 2.1 for electric pumps and 1.1 for diesel/gas powered pumps to the energy consumption per load range values.

Table 4.34 The primary energy consumption per payload range of oil and gas pipeline

Oil and gas pipeline	$E_{prim}/(s \cdot m_{pl})$ (electric) J/mkg	$E_{prim}/(s \cdot m_{pl})$ (diesel/gas) J/mkg
Water pipeline	0.29	0.51
Heavy oil pipeline	0.69	1.20
Gas Pipeline	1.69	2.95

5 Results and Discussion of New Karman-Gabrielli Diagrams

Efficient and cost-effective transportation is desirable. Achieving economic efficiency involves minimizing drag, reducing energy consumption during operation, and reducing emissions. This study will therefore utilize two properties: speed along the x axis, lift-to-drag ratio and inverse primary energy along the y axis. The objective is to achieve a higher lift-to-drag ratio and speed, while inversely reducing primary energy consumption.

5.1 KG Diagram: Lift over Drag
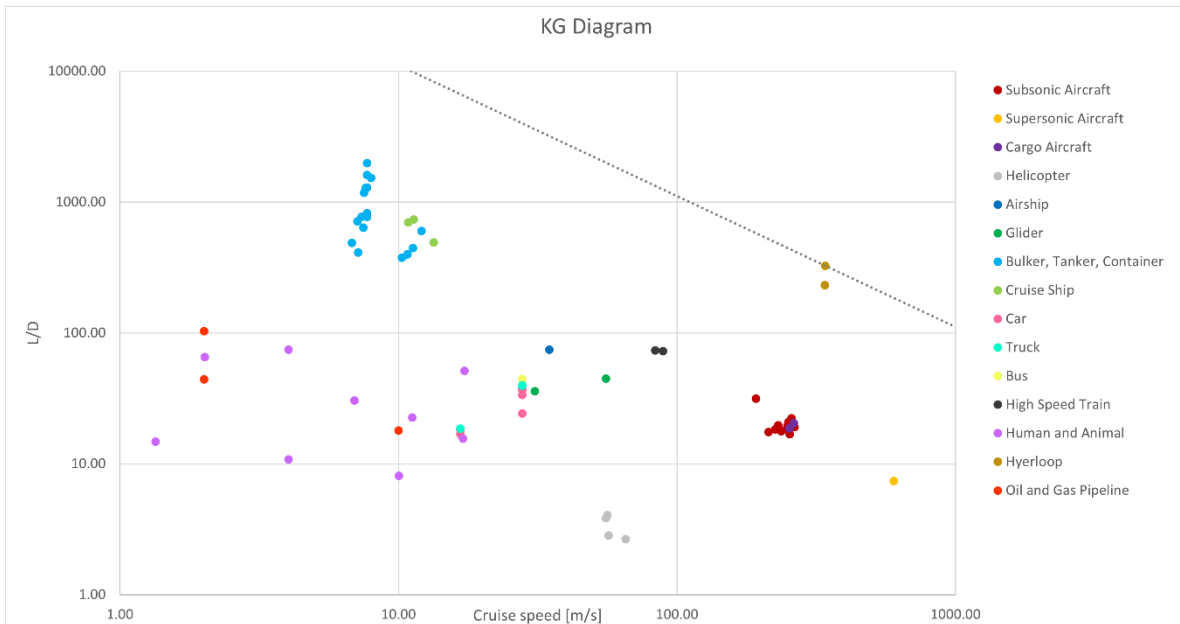
Figure 5.1   Karman-Gabrielli diagram for all vehicles

The log-log plot presented in Figure 5.1 illustrates the relationship between lift-to-drag ratio $\frac{L}{D}$ and cruising speed V for various modes of transportation. The depicted line in the diagram denotes the Hyperloop transportation figure of merit, which serves as a compromise border line. The transport figure of merit, denoted as a_{LD}, can be obtained by multiplying the lift-to-drag ratio with the cruise speed (Appendix A). The increase in speed results in a reduction of the lift-to-drag ratio. Consequently, it is possible for vehicles possessing identical transport figures of merit yet varying lift-to-drag ratios to exhibit the same lift-to-drag ratio, given that the speed of one of the vehicles is elevated.

In comparison to other modes of transportation, ships exhibit a superior lift-to-drag ratio, however, when compared to the Hyperloop, their velocity is relatively sluggish. The

aforementioned statement implies that ships have the capacity to transport larger quantities of cargo albeit at a comparatively lower velocity, whereas aircraft are limited in their cargo capacity and can only transport smaller loads at higher speeds. Nonetheless, it shouldn't be taken as a given that other modes of transportation with a lower transport figure of merit ought to be disregarded. Each possesses distinctive characteristics and advantages. Helicopters are capable of flying at low altitudes, making them suitable for short-range missions, and they possess the ability to land on narrow terrain. Cars exhibit a commendable level of transportation efficiency when travelling both urban and rural thoroughfares. But only when the vehicle is completely occupied. The transportation of goods and individuals through the utilization of human and animal labor is limited to brief distances and minimal weights.

A further review about lift-to-drag ratio and cruise speed was done specifically for aircraft, where the diagram was made to resemble the Pareto front diagram. The collection of parameterizations or allocations that exhibit Pareto efficiency within a particular system is commonly referred to as the Pareto front. The identification of Pareto boundaries holds significant utility in the field of engineering (Wikipedia 2023m). By limiting the set of parameters, a designer can make focused decisions and generate all feasible optimal solutions, without the need to consider the entire range of parameters. Solutions that lie on the objective line are considered to be optimal or Pareto efficient. Objective line in this paper pertains to the transport figure of merit, however not in the log-log plot. Figure 5.2 displays several iterations of the Pareto front. The distinct hues present on each diagram denote the objective line, which designates the Pareto optimal solution.
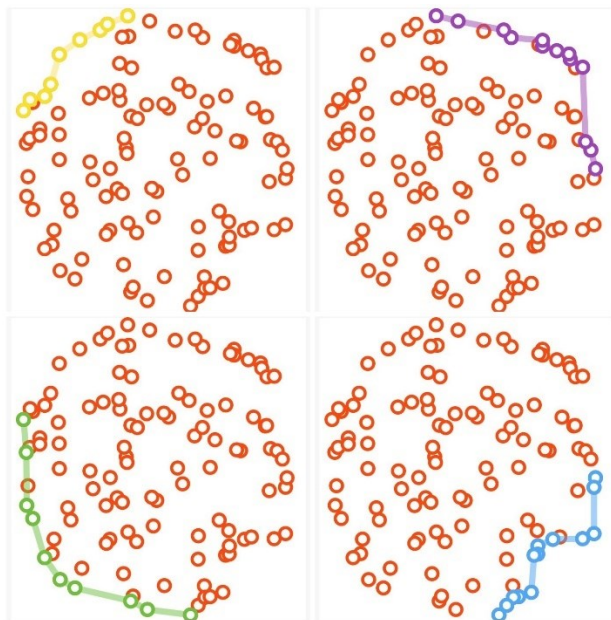

Figure 5.2   4 variants of the Pareto front

Basically, the transport figure of merit a_{LD} is achieved by multiplying the cruise speed and lift-to-drag ratio, where in the Figure 5.1 displayed as x-axis and y-axis.

$$a_{LD} = x \cdot y \tag{5.1}$$

Regrettably, a mere alteration of the axis from logarithmic to linear in the Karman-Gabrielli diagram fails to bear resemblance to the Parent front diagram, as the solution falls beyond the objective curve or objective line. To achieve the objective line in desired graph as in Figure 5.2, the x-axis and y-axis are inverted. The initial step involves the inversion of the y-axis y', so (5.1) will be as follows,

$$y' = \frac{x}{a_{LD}} \tag{5.2}$$

Then the x-axis is also inverted,

$$y' = \frac{1}{x' \cdot a_{LD}} \tag{5.3}$$

Ultimately the objective line or transport figure of merit is the multiplication of two axes.

$$a_{LD} = \frac{1}{x' \cdot y'} \tag{5.4}$$

The utilization of the weighted sum approach is deemed unnecessary in this study, as the objective function is exclusively composed of the product of the x-axis and y-axis. Furthermore, the number of solutions presented in this the paper is fewer in comparison to those depicted in Figure 5.2. Consequently, the methodology employed to generate the objective line is predicated on the most efficient vehicle.

The decision to prioritize either speed or lift-to-drag ratio can be viewed as a philosophical one, as each potential solution to the objective function yields a transport figure of merit that is equally effective. Simultaneous attainment of the maximum value for both variables is not possible.

In Figure 5.3, the objective curve is obtained from the inverse transport figure of merit of the YB-49 aircraft because its transport figure of merit value is the largest. There is also a Concorde on the other side of the curve. If these two aircraft are compared, YB-49 has a greater lift-to-drag ratio than Concorde, it is due to its larger wing size that produces greater lift. But on the other hand, Concorde has a fast cruising speed but relatively low drag because of its delta wing, even the fastest compared to other aircraft. Another aircraft that is also close to the curve is the A340-300. Compared to the YB-49, it has a faster cruising speed, and when compared to the Concorde, its lift-to-drag ratio is greater. In other words, the aircraft is relatively faster with a relatively larger carrying capacity. It can also be seen in the diagram that many passenger aircraft that are relatively frequently operated today are around the A340-300 point. This is because passenger aircraft will be optimal if they have a good speed

rate and ligt-to-drag ratio. Another aircraft that is clearly dominated is the helicopter. Compared to fixed-wing aircraft, helicopters are slower, but they are more versatile and can land anywhere quickly. Since this paper is specific to cruising speed and lift-to-drag ratio, choosing between helicopter or fixed-wing aircraft is a technical decision for engineers rather than a philosophical decision.
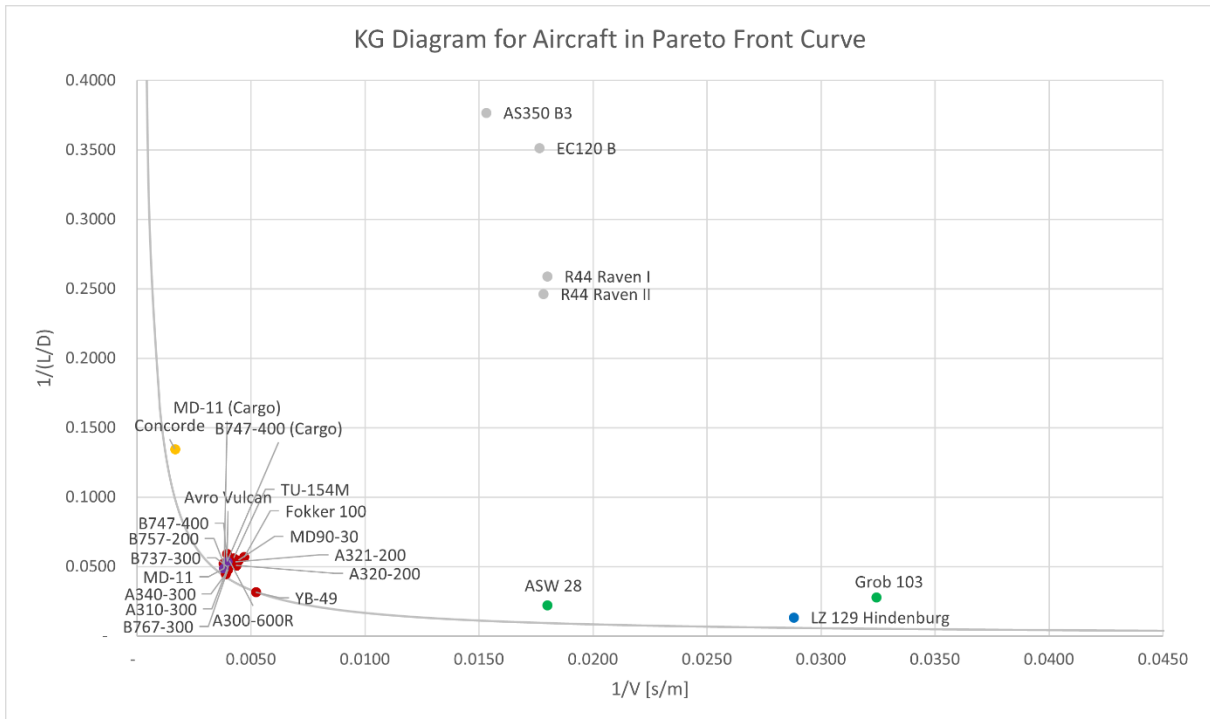
Figure 5.3   Karman-Gabrielli diagram for aircraft in Pareto front curve

5.2   KG Diagram: Payload Fraction times Lift over Drag

Although some vehicles may have a favourable lift to drag ratio, they may also have heavy vehicle body weight and have limited capacity. That is why the idea of the diagram in Figure 5.4 produced. It shows the log-log plot of lift-to-drag ratio regarding payload mass $\left(\frac{L}{D}\right)_{pl}$ versus cruising speed V.

A noticeable decrease in the transport figure of merit of certain vehicles is evident upon comparing Figure 5.4 with Figure 5.1. This phenomenon can be attributed to the relatively low ratio of payload mass in comparison to the overall mass. The vehicle's heavy weight limits its capacity to carry a small payload. Undoubtedly, in the context of transportation, such occurrences must be circumvented. Opting for a vehicle with a high payload capacity and low weight is considered advantageous. A cruise ship's payload is relatively small in comparison to its overall weight due to the presence of numerous amenities for passengers, including to swimming pools, casinos, fitness centers, spas, and cinemas. The inherent

purpose of a cruise, which is to provide a leisurely and enjoyable experience, coupled with the willingness of passengers to pay a premium for enhanced comfort and an extended holiday, precludes it from being directly analogous to ICE. The primary objective of an ICE or aircraft is to efficiently transport passengers at a reasonable cost.
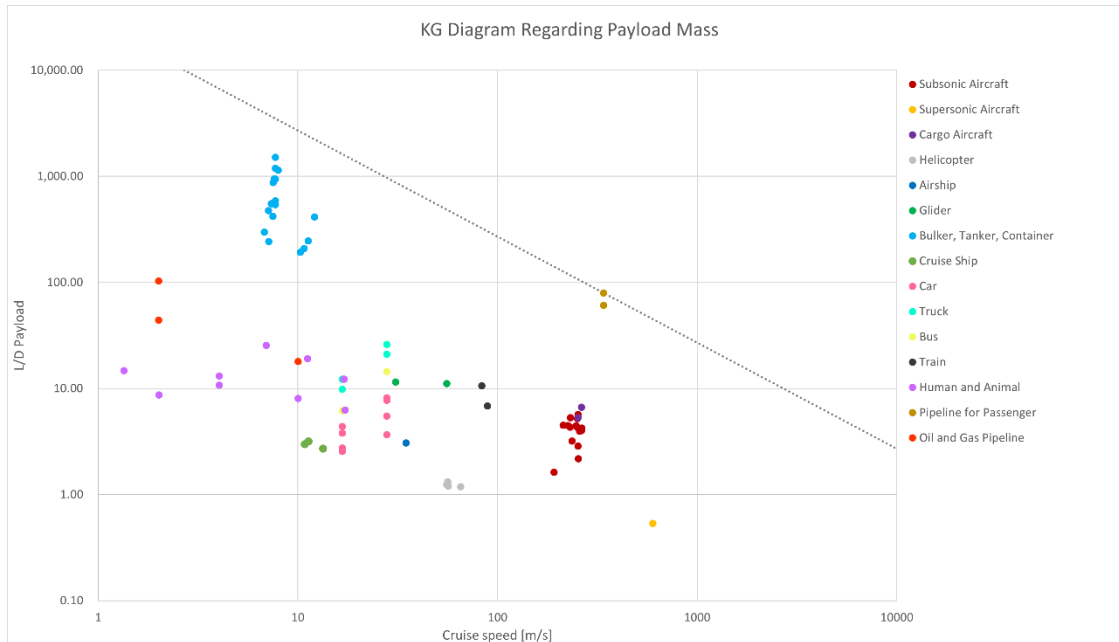
Figure 5.4   Karman-Gabrielli Diagram regarding payload mass for all Vehicles

The transportation of freight can be categorized into various modes such as bulker, truck, cargo airplane, and oil and gas pipeline. It has been observed that among these modes, vessel transportation exhibits the highest lift to drag transport figure of merit. Nevertheless, the comparatively lower velocity of bulk carriers in contrast to trucks and aircraft represents a drawback. The transportation of perishable items, such as fish and flowers, will be of utmost importance. Opting for a slower transportation method, as opposed to air cargo, may result in the deterioration of perishable goods such as fish and flowers. In the event that time-sensitive perishable goods require transportation, the most viable options would be hyperloop and aircraft due to their high cruising velocities. Figure 5.4 illustrates that the transport figure of merit of the hyperloop system surpasses that of aircraft and outperforms other modes of transportation. This paper states that the cargo hyperloop has the capacity to transport both cargo and passengers concurrently, whereas air cargo exclusively transports cargo. Thus, if the primary objective is solely to transport freight at a higher speed, then the airplane is a viable option.

Despite the relatively low velocity of oil and gas pipeline transportation, the lift-to-drag ratio remains reasonable and comparable to that of the hyperloop. The issue of slow loading speed may not be a significant concern, as oil and gas commodities are non-perishable and operational hours are not constrained by human working hours, unlike in the case of trucks where drivers require breaks for eating and rest.

The passenger hyperloop transport figure of merit is considered the most optimal means of transportation for passengers. On average, the capsules depart from each terminal after a duration of 2 minutes, accommodating 28 individuals per capsule (Musk 2013). Given the current absence of a commercial hyperloop, alternative options for high-speed transportation include high-speed trains and aircraft. Undoubtedly, airplanes exhibit greater speed than high speed trains; however, high speed trains possess the capacity to accommodate a larger number of passengers. Airplanes are recommended for long-distance travel over bodies of water, whereas high-speed trains are designed for destinations that are accessible via railways. Long-distance buses are a viable mode of transportation for passengers, as they offer a lift-to-drag ratio that is superior to that of high-speed trains and aircraft. The sole disadvantage is that the velocity is comparatively lower. Therefore, utilizing buses as a means of transportation for passengers between cities is a viable solution.
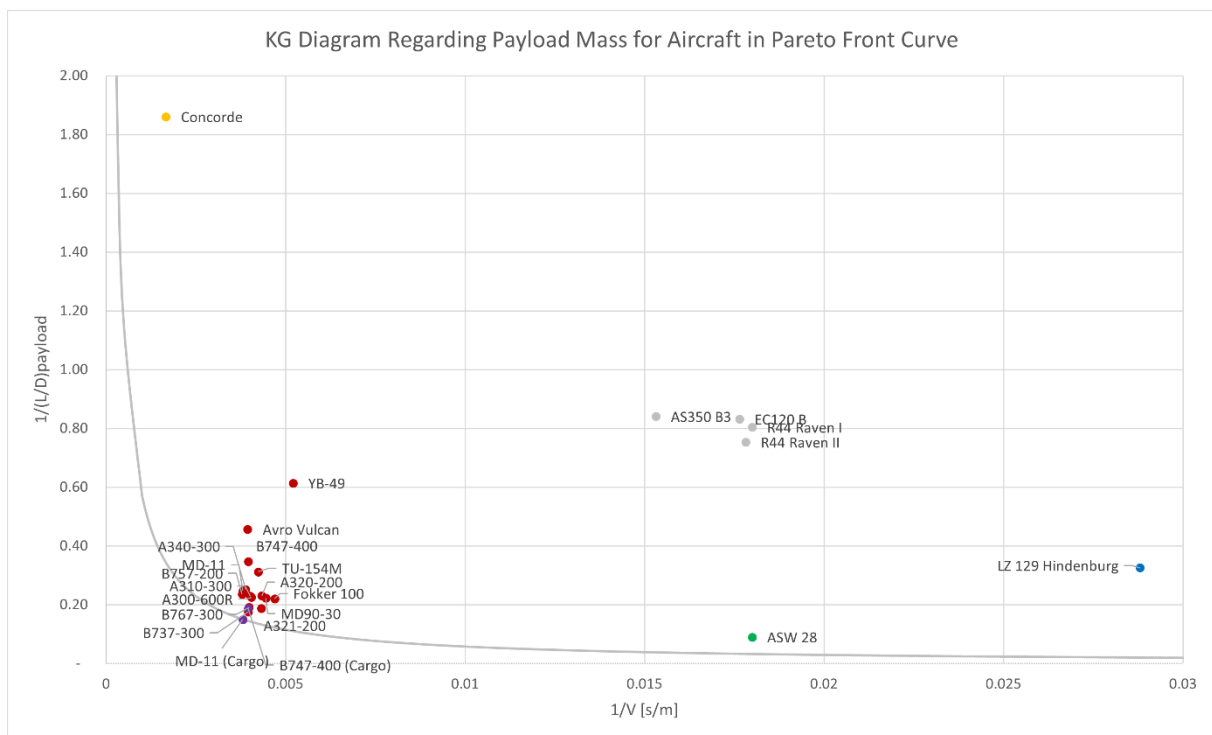
Figure 5.5   Karman-Gabrielli Diagram regarding payload mass for aircraft in Pareto front curve

In greater depth, when examining aircraft, it becomes apparent that if a cargo airline is situated in the objective line, it possesses the highest transport figure of merit. This outcome is a direct result of the primary function of cargo airlines, which is to transport goods, thereby resulting in a relatively large percentage of payload to total mass. The Karman-Gabrielli diagram in relation to payload mass reveals that the YB-49 no longer holds the highest transport figure of merit as to be seen in Figure 5.3. The YB-49 is characterized by a significant lift capacity, attributable to its expansive wingspan. However, its payload capacity is comparatively limited in relation to the overall weight of the aircraft, including both its basic empty weight and fuel load. An additional factor to consider is that the YB-49 is classified as a bomber aircraft, designed solely for military purposes and not intended for the

transportation of passengers or cargo. As a result, it is reasonable to expect that the proportion of payload weight to the overall mass of the aircraft would be relatively low. Similarly, the Avro Vulcan, which was also utilized as a bomber, exhibited this characteristic.

The highest transport figure of merit among passenger aircraft belongs to the B737-300 in the narrow body class and the B767-300 in the wide body category. In the Airbus aircraft lineup, the A321-200 narrow body and the A300-600R and A310-300 wide bodies are rated as the best transport figures of merit. Additionally, the typical cruise speed of Airbus aircraft is higher than that of Boeing aircraft. Large, double-decker airplane with a high passenger capacity is the B747-400. However, despite its large passenger capacity, the aircraft's heavy weight results in a small proportion of payload relative to its total mass and a moderate cruise speed, giving it a low transport figure of merit in comparison to other passenger aircraft.

In the context of airships, particularly LZ 129 Hindenburg, the lift-to-drag ratio pertaining to payload mass exhibits a significantly lower value compared to the lift-to-drag ratio associated with total mass. The substantial mass of hydrogen and its corresponding envelope result in a relatively dropped proportion of payload allocation from the total mass. In other terms, only a limited payload can be carried by a substantial mass.

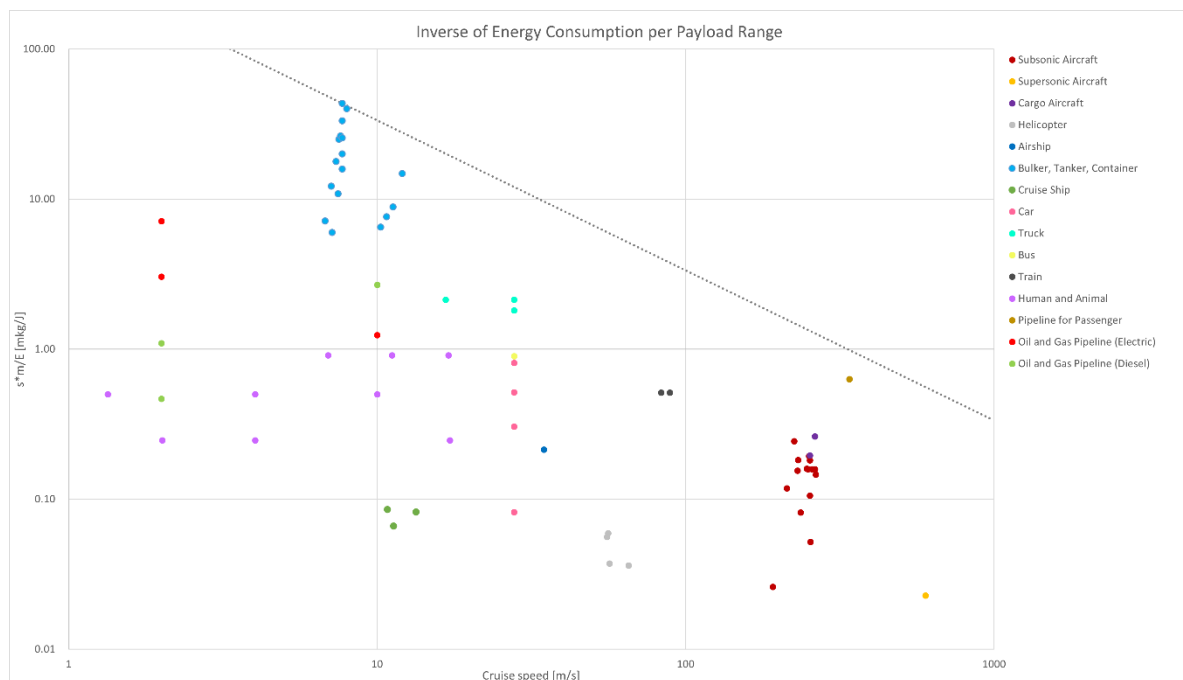## 5.3 KG Diagram: Inverse of Energy Consumption per Payload and Range

Figure 5.6 Inverse of energy consumption per payload and range for all vehicles

If the modes of transportation are examined in terms of their energy consumption, Figure 5.6 shows the inverse of energy consumption per payload and distance travelled. In general terms, the inverse consumption per payload and range diagram bears resemblance to the Karman-Gabrielli diagram illustrated in Figure 5.1. But there have been significant changes as the compromise boundary is now bulker instead of hyperloop. In comparison to a bulker, the energy consumption required for the transportation of passengers and payload is higher in the case of hyperloops.

Notable alterations are observed on the cruise ship's position, which has shifted considerably lower than the bulker. This is in contrast to the depiction in Figure 5.1, where the cruise ship remains within the same area as the bulker. The veracity of this claim has been established in Figure 5.4, where the low payload of the ship is attributed to the weight of the facilities provided for passengers during the journey. Another crucial aspect to consider is the significant amount of power required to operate these facilities. Various amenities such as lighting and sound systems for stage performances, electricity to power theaters, restaurant necessities, and air conditioning units strategically placed to ensure passenger comfort are essential components of modern infrastructure.

Passenger vehicles that utilize fuel and operate at comparable velocities include cars and buses. As a result, it can be observed that buses necessitate a lower amount of energy to transport their payload. Therefore, utilizing a bus as a mode of transportation is more advantageous compared to utilizing a personal vehicle such as a car. If the energy required is reduced, then the fuel consumption per unit of payload and range is correspondingly decreased, resulting in a reduction in fuel expenses.
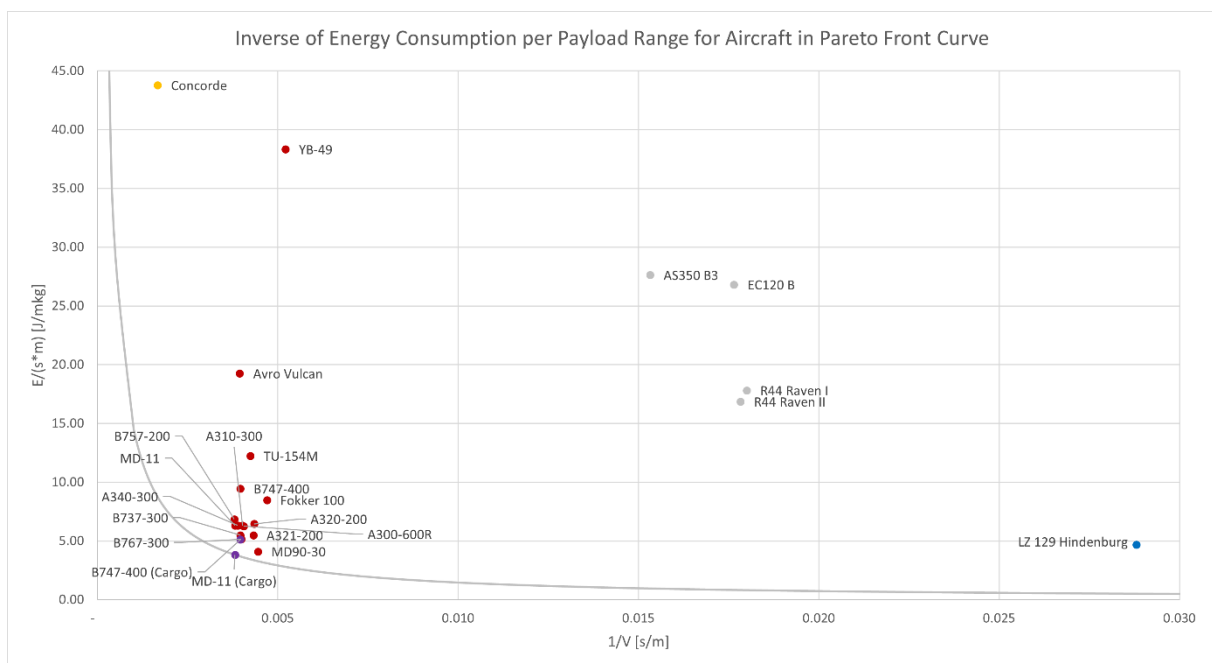

Figure 5.7   Inverse of energy consumption per payload and range for aircraft in Pareto front

Upon closer examination of the aircraft categories presented in Figure 5.7, it is evident that cargo aircraft, particularly those utilizing the MD-11 aircraft, exhibit the lowest energy consumption levels when transporting their cargo. In the domain of aviation, the energy consumption pertaining to aircrafts is associated with the lift-to-drag ratio, as per the formula delineated in (3.4) for the computation of specific air range (SAR). It is noteworthy that SAR is the reciprocal of fuel consumption. A higher lift-to-drag ratio is positively correlated with an increase in specific air range (SAR) and a decrease in fuel or energy consumption. In addition to the lift-to-drag ratio, the SAR is also influenced by the specific fuel consumption parameter, denoted as c. A higher SAR is associated with a lower specific fuel consumption. The specific fuel consumption pertains to the amount of fuel consumed by an aircraft engine per unit thrust, and is subject to the influence of various factors related to the engine, including the bypass ratio (BPR). An engine possessing a high bypass ratio has the capability to produce greater thrust than an engine with a low bypass ratio while utilizing an equivalent amount of fuel (Dankanich and Peters 2017). The YB-49 aircraft serves as an illustrative instance. The lift-to-drag ratio value of the aircraft is commendable; however, due to the presence of a solitary flow turbo jet engine, the bypass ratio (BPR) value is rendered null which then it can be inferred that the aircraft has a high energy consumption rate for its operation.

The Concorde exhibits a relatively elevated energy consumption in relation to its payload and range. The reason for this is due to its ability to operate at a significantly higher velocity than that of subsonic commercial airplanes, and its utilization of four engines based on military technology. Additionally, the percentage of passenger capacity is lower compared to that of subsonic passenger airplanes.

Theoretically, an increase in the number of engines results in a corresponding increase in fuel consumption. But the utilization of additional engines results in an increased capacity for carrying weight, as a consequence of the requirement for thrust in generating lift. The B747-400 exhibits high energy consumption per unit payload and distance due to its 4 engines and the small percentage of payload to total mass, as depicted in Figure 5.7. In comparing two aircraft that utilize four engines, it has been observed that the A340-300 outperforms the B747-400 in terms of energy efficiency with respect to payload and range. This is attributed to the A340-300's engine having a smaller specific fuel consumption as compared to the B747-400, despite the payload mass to total mass ratio being similar for both aircraft.

The glider has been excluded from the diagram due to its non-reliance on fuel or engines for operation, thereby rendering energy consumption irrelevant. The LZ 129 Hindenburg exhibits low energy requirements for cargo transportation, yet with a notably slow cruising velocity.

The utilization of energy has a direct effect on the consumption of fuel, subsequently influencing the expenses incurred in operations. Nevertheless, mere computation of energy usage is insufficient; a thorough analysis of primary energy consumption is imperative.

5.4   KG Diagram: Inverse of Primary Energy Consumption per Payload and Range
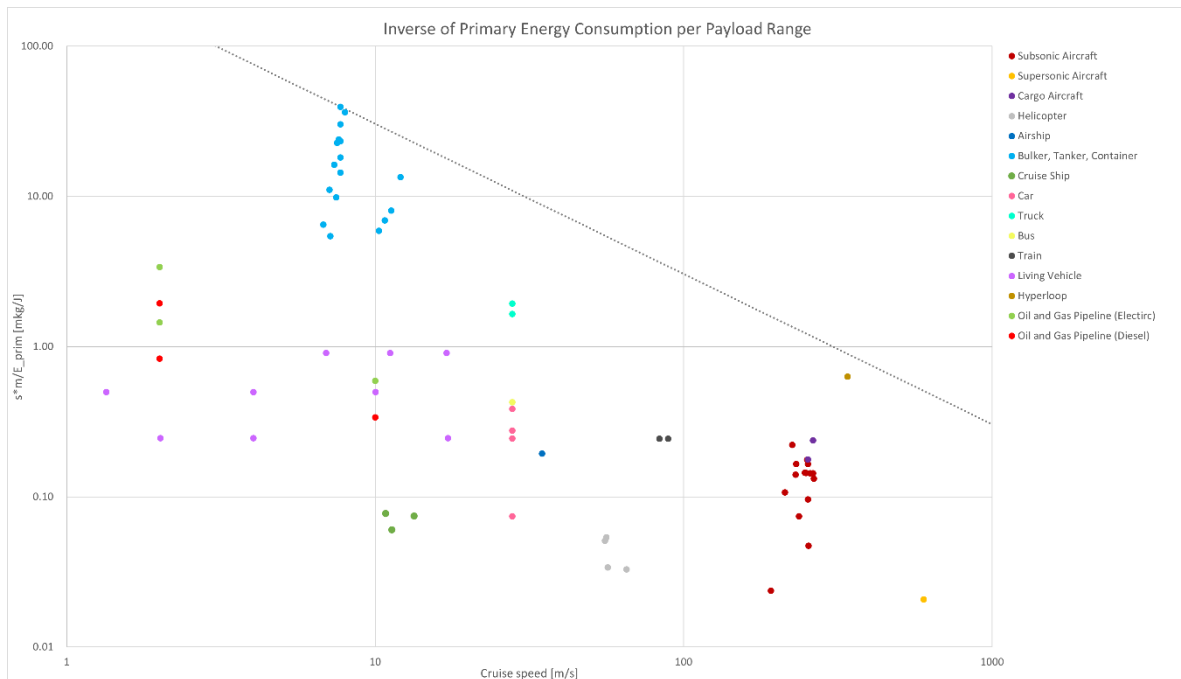
Figure 5.8   Inverse of primary energy consumption per payload and range for all vehicles

The primary energy of vehicles utilizing kerosene or diesel fuel can be determined by applying a multiplication factor of 1.1, which accounts for the 10% of fuel that is consumed during the refining process. Electrically-operated vehicles are multiplied by a factor of 2.1. The aforementioned factor represents the primary energy factor for electricity in the year 2023, exhibiting a consistent annual decline (Scholz 2019). The transport figure of merit of trains is comparatively lower than the figures depicted in Figure 5.1 and Figure 5.4. This can be attributed to the fact that trains, particularly those that operate at high speeds, rely on electric power for their operation. Despite the fact that high speed trains exhibit a relatively higher energy consumption per payload and range compared to aircraft, they remain the most prevalent mode of transportation due to their eco-friendliness, as they rely on green power. As of 2018, all ICEs operating in Germany are powered exclusively by renewable energy sources (Deutsche Bahn 2023).

From Figure 5.8, it can be analysed that the average freight transport has a relatively high transport figure of merit a_E, such as vessels, trucks, air cargo, and also oil and gas pipelines. As a freight transport, the oil and gas pipeline transport tends to have a lower transport figure of merit in regards to energy than bulker and air cargo. But so far, it is a favourable means of transportation, especially for delivering oil and gas within continents. This is due to its ability to deliver goods continuously without any other obstacles from the environment because the pipeline is embedded in the ground. While bunkers, trucks, and planes have a better transport figure of merit than oil and gas pipelines, the cost of operation will be higher because during a

journey, many other cost components must be charged where oil and gas transport does not. While the transportation of oil through pipelines may require a greater amount of energy, particularly if diesel fuel is utilized, it is a more cost-effective method due to its ability to accommodate large volumes, particularly when cooling is implemented during operation, resulting in a significant reduction in gas volume for transmission (Wagner 2017). This has a correlation with Direct Operating Cost (DOC) whose components can be described in the following formula (Scholz 2015).

$$C_{DOC} = C_{DEP} + C_{INT} + C_F + C_M + C_C + C_{FEE} \qquad (5.1)$$

In its application to the freight transport category, oil and gas pipelines can deliver goods without charging crew fees C_C during cruise. The cost of maintenance C_M is relatively low because the components are not as complex as those of aircraft or ships. Because the pipeline is buried underground, it will not interfere with nearby activities and is exempt from fees and charges C_{FEE} such as landing fees and air traffic control or navigation fees. Conca (2014) can further clarify that crude oil pipeline transport costs approximately \$5 per barrel, but rail transport costs \$10 to \$15 per barrel and trucking has significantly greater expenses due to the need for additional manpower; employment on completed pipelines is just "1 percent of that of the trucking business." The illustration depicts a pipeline for oil and gas transportation that employs either diesel fuel or electricity as a means to power its pumps. The pump's efficiency is measured at 0.75 (Kollmar 2023) . In the event that the pump is utilized with gas or fuel sourced from the pipeline, which exhibits an efficiency of 0.3, the energy consumption is then amplified by a factor of 4.4.

Even so, the oil and gas pipeline continues to be a subject of debate when compared to bulkers, tankers, and container vessels, as it is constrained to the transportation of gas and liquids exclusively. Bulkers, tankers, and container vessels exhibit greater transport efficiency compared to pipeline transportation.

When comparing a car with a helicopter, they have similar transport figures of merit, but the helicopter has a greater cruising speed and the car has a better energy consumption per unit range and payload. The speed relates to the value of time, the opportunity cost of the time a traveler spends on their trip in the context of transportation economics. Value of time can be categorized for both types of valuations, namely working time and non-working time. Working time values are time spent traveling during the working day. From an employer's perspective, the act of traveling during working hours represents a cost, as the time spent traveling could otherwise be utilized for productive purposes. In the given scenario involving helicopters and cars, it is recommended that employees opt for helicopter transportation as it offers a quicker means of reaching the intended location. The cost per hour of utilizing a helicopter is comparatively higher than that of a car, as it entails a greater spending in order to reduce on travel time. The salary rate paid to workers is indicative of the significance assigned to their working time. In the context of car transportation, a distinction is made between individuals who assume the role of a driver and those who occupy the position of a passenger. The value of time differs between car drivers and car passengers, as passengers

have the chance to engage in work-related activities during the journey, whereas for car drivers, the time spent traveling is unproductive (Wikipedia 2023n).

Upon further elaboration, it can be observed that there exists a direct relationship between drag, energy consumption, and the value of time. Specifically, drag and energy consumption exhibit a proportional relationship to the square of the speed, while the value of time is directly proportional to the speed[4]. In considering the observed effect of increased drag, it may be inferred that a mode of transportation characterized by high velocity would exhibit inferior performance relative to a slower alternative with the same transport fisgure of merit. In this particular scenario, it can be argued that cars are a superior mode of transportation to helicopters due to the fact that the helicopter generates a significantly higher amount of drag, approximately four times more, than the car. Additionally, the time value of utilizing a helicopter is only twice that of using a car. Rather than enhancing the value of time through escalated speed, the drag and energy usage experience a surge.
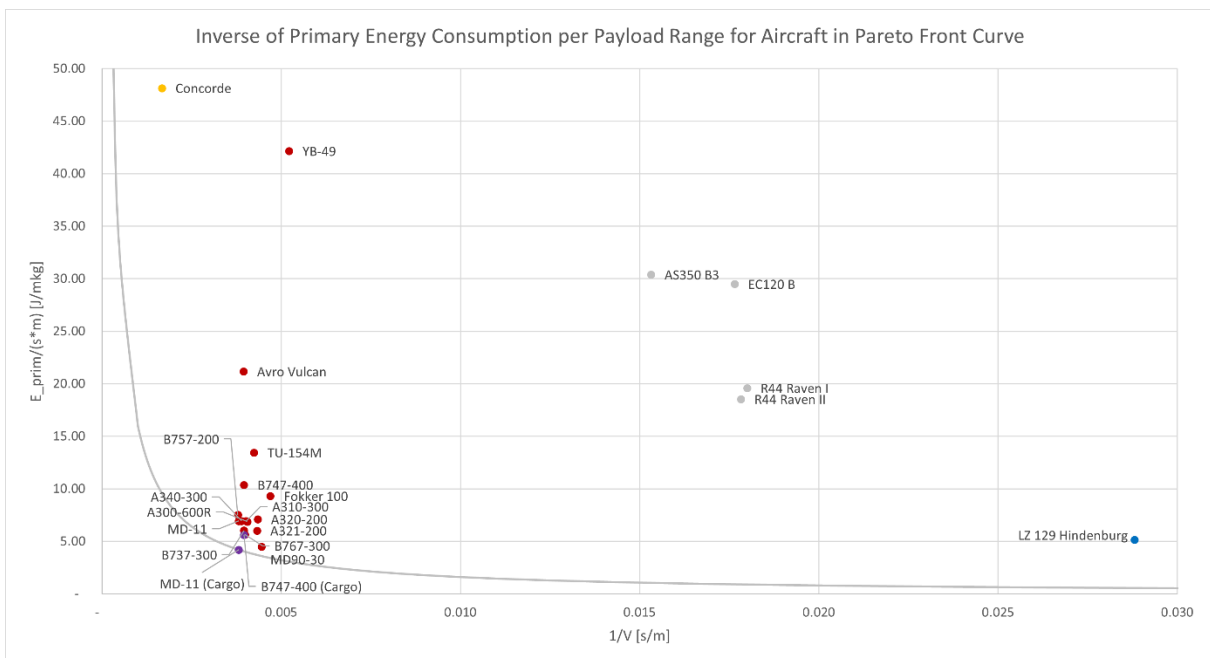
Figure 5.9 Inverse of primary energy consumption per payload and range for aircraft in Pareto front

The inverse of energy consumption per payload and range for various aircraft is depicted in Figure 5.9. The outcome is equivalent to that of Figure 5.7, as it has been scaled by a factor of 1.1.

The source of energy utilized for vehicular operation is either fuel or electricity, both of which are not exempt from the potential of emitting emissions, as it leads to the production of carbon dioxide emissions. Carbon dioxide emissions are a byproduct of the combustion of fossil fuels.

---

[4]   Prof. Scholz's explanation during thesis supervision, sent through his email.
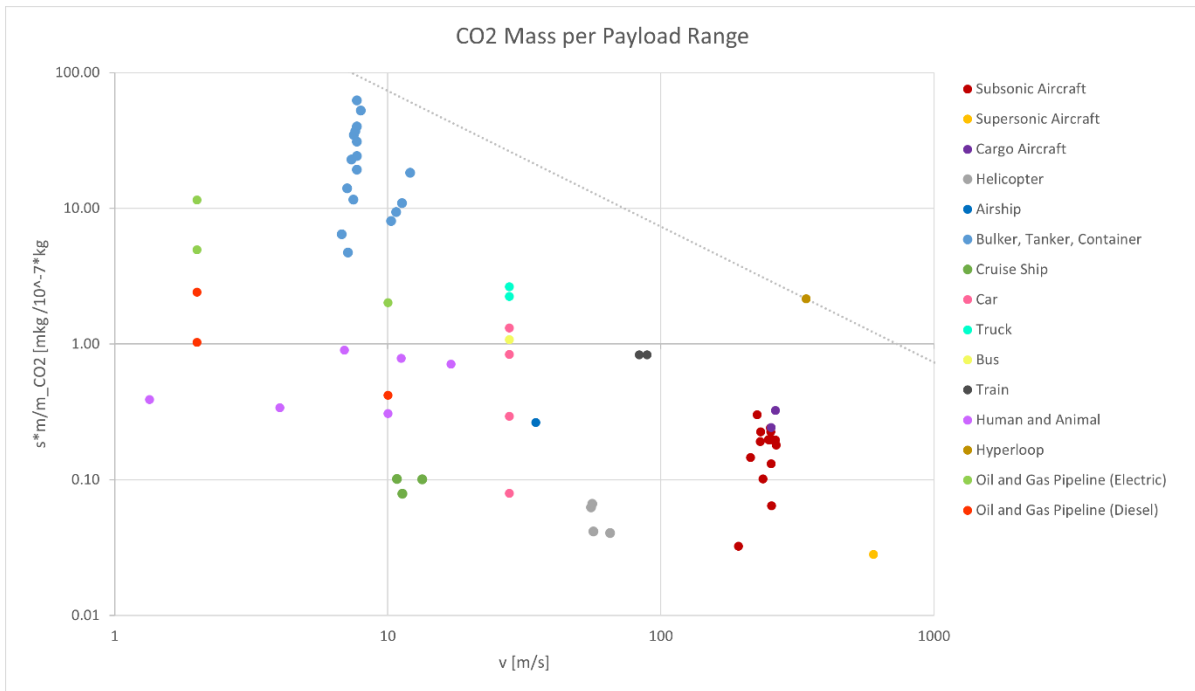
Figure 5.10   Inverse of CO2 mass to payload and range

The inverse of carbon dioxide emission per payload and range for all vehicles is illustrated in Figure 5.10. The computation can be bifurcated into two distinct categories, namely for vehicles that are powered by diesel fuel and those that rely on electricity as their source of energy. In the case of gasoline-powered vehicles, it is necessary to apply a multiplication factor of 3.5 to the fuel mass, as well as a factor of 1.1. The utilization of factor 1.1 has been employed in the computation of primary energy utilization. This factor represents 10% of the fuel combusted in the refinery during the production of fuel. The emission index of CO2 is denoted as 3.15 and is defined as the ratio of kilograms of CO2 emitted per kilogram of fuel (Scholz 2019). In the case of an electrically-powered vehicle, it is necessary to apply a multiplication factor of 3.15 to the primary energy consumption, and subsequently multiply this value by x_{ff}. Finally, the resulting figure must be divided by the heating value of kerosene. The value of x_{ff} is 0.4, suggesting that the source of electricity comprises not only fossil fuels but also renewable energy and nuclear power sources. To convert from electrical energy to fuel energy, assuming that all electricity is generated from fossil fuels, one must divide primary energy consumption by the heating value of kerosene.

In terms of carbon emissions, vessels exhibit the lowest levels of CO2 per payload and range output relative to other modes of transportation, while conversely, cruise ships are associated with the highest levels of CO2 emissions. The aforementioned phenomenon has the potential to inflict harm upon the marine ecosystem. This is due to the fact that the ocean has the capacity to assimilate as much as 40 percent of carbon dioxide. As the concentration of CO2 increases, the acidity of the ocean is likely to intensify, thereby leading to the deterioration of coral reefs (CRA 2023).
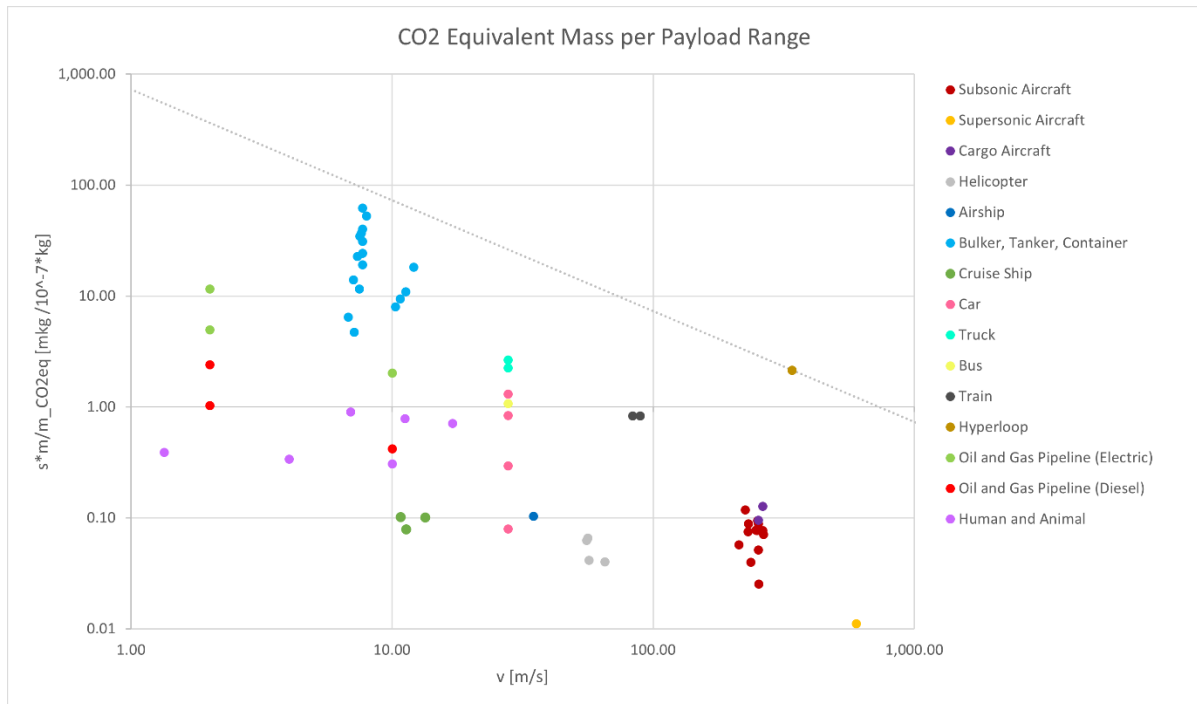
Figure 5.11   Inverse of equivalent CO2 mass to payload and range

The mode of transportation that has the most significant carbon dioxide equivalent emissions impact is the airplane. In addition to their emissions of vapor trails, aircrafts also make a contribution to the release of nitrogen oxide (NOx). The radiative forcing index, with a value of 2.7, is a contributing factor to the determination of equivalent CO2 mass. The aforementioned statement implies that the impact of air traffic on global warming is 2.7 times more significant than the actual carbon dioxide emissions produced by aircraft. This is also due to the altitude effect. At specific elevations, the emission of NOx leads to a higher concentration of O3 compared to NOx emissions at ground level, thereby causing a more significant impact on global warming (Schumann 2002).

The domain of freight transportation can be classified into three distinct categories, namely air transportation which involves the use of planes, land transportation which involves the use of trucks, and sea transportation which involves the use of vessels. When making a comparison, it is evident that airplanes are the least favorable option in regards to its emission, while trucks fall in between airplanes and vessels. The greater the distance travelled, the higher the resultant greenhouse gas emissions. Hence, trucks would be the optimal option for transporting goods over short distances. The larger the vehicle, the greater its capacity for transporting goods, resulting in a more favorable greenhouse gas balance.(link umwelt). Vessels can be regarded as environmentally sustainable due to their minimal emission of carbon dioxide. This phenomenon can be attributed to the reduced velocity and incomplete power output, resulting in fuel conservation and a decrease in CO2e emissions. A reduction in ship velocity by 10% is expected to result in a total reduction of 19% in carbon dioxide emissions (Transport Environment 2023). Despite its low operational cost and environmentally friendly nature, prudent operation is still necessary to avoid excessive non-essential trips.

The hyperloop is a novel mode of passenger transportation that boasts both high speed and environmental sustainability. The reason for this is that the system employs sustainable energy sources, specifically solar panels, to power its operations during daylight hours, and subsequently stores this energy in batteries for use during night time hours. However, it should be noted that the aforementioned mode of transportation is not currently accessible to the wider public. Furthermore, even in countries where it is available, its reach is limited. The implementation of this technology in other countries is expected to be an exhaustive procedure due to the complex process of its construction, which involves subterranean embedding and considerable length. The fundamental concept underlying hyperloop technology is akin to that of oil and gas pipelines. However, it is imperative to underscore the crucial role of ensuring safety in hyperloop systems, given the importance of human safety. Notwithstanding the challenges encountered in the manufacturing process, the product's delayed release is justified by its environmentally sustainable nature and favorable lift-to-drag ratio.

Long distance passenger transportation is frequently facilitated by buses and high speed trains, which are known to generate the lowest equivalent CO2 mass when compared to other modes of transportation, such as aircraft and cruise ships. Figure 5.11 illustrates that the high-speed train outperforms the bus in terms of passenger transportation emissions due to its utilization of renewable energy as its electrical power source. Long distance bus presents a favorable option in terms of emissions due to its commendable ecological balance and high capacity utilization, despite its non-reliance on renewable energy sources. The singular disadvantage is that it does not possess the same level of speed as high speed trains or aircraft.

Cars and helicopters are viable transportation options for covering short distances. Cars are a viable option, particularly in the context of electric vehicles. Due to their practicality as a mode of transportation and the inherent privacy they provide, a significant number of individuals favor the use of cars over public transportation. The impact of the operation of helicopters is not as direct as that of cars, as helicopters require specialized skills to operate and are not accessible to everyone. Additionally, the runway for helicopters is typically located in open areas with lower population density, as opposed to the residential areas where cars are commonly used for daily activities. Helipads are commonly situated atop high-rise structures even in regions with high population density. The comparison between rotary wing aircraft and fixed-wing aircraft cannot be made on the assumption of altitude as the helicopter does not operate at high altitudes. Consequently, the CO2e mass value of rotary wing aircraft remains unaffected by the radiative forcing index.

Walking and cycling are frequently regarded as sustainable transportation options due to their environmentally conscious nature. According to Figure 5.11, the CO2e emissions resulting from human walking and cycling are lower than those of the car with the highest emissions, when considering only the equivalent mass of CO2 produced during the trip. However, when taking into account the CO2e emissions per unit payload and unit range, the car average value performs better. From a certain perspective, it can be argued that a fully occupied car emits a lower amount of CO2e per unit of payload transported compared to human walking, as a

larger amount of payload can be transported in a single trip. In comparison to electric vehicles, walking or biking results in a higher emission of equivalent carbon dioxide. Despite not being a direct contributor, humans generate a significant amount of carbon dioxide through various means. The acquisition of human energy is reliant upon the consumption of food, which in turn necessitates a series of processes that generate carbon dioxide emissions. This phenomenon is a result of the food chain. As an illustration, cow serve as a source of energy for human consumption. Cows emit various types of gases that possess a greater degree of harmfulness than carbon dioxide. It has been observed that a single cow can generate a greater amount of emissions compared to a car, particularly considering the global population of cows surpasses that of cars (McKenzie 2013). Figure 5.8 also shows that human walking and biking require more energy to move their payload than other forms of transit, which is another argument in favor of how much CO2 is produced by these activities.

6 Conclusions and Recommendations

6.1 Conclusions

The objective of this study is to evaluate the efficacy of a transportation mechanism for carrying payload under varying speeds, with a focus on lift-to-drag ratio and primary energy consumption. The speed at which an individual travels has an impact on their value of time during transportation. The inquiry pertains to whether people would opt to allocate extra money to minimize time spent on a journey, or alternatively, would choose to invest more time in order to reduce monetary expenditures.

When comparing vehicles within the same category, the distinguishing factors are typically their features and dimensions. An analysis of the B747 aircraft in comparison to other aircraft models. The B747 aircraft exhibits a suboptimal lift-to-drag ratio and a relatively high primary energy consumption per unit payload and range. Despite its heavy body and a relatively small percentage of payload in total mass, the B747 is capable of transporting a greater number of passengers compared to other aircraft. Similarly, the four engines necessary to support such a substantial mass are capable of achieving flight at higher altitudes due to the need for thrust to generate lift. Flying at greater heights corresponds to increased velocity, as the air is less dense.

However, when comparing various vehicle types, the vehicle's performance will vary due to the fundamental physical principles employed. The operational performance of a vehicle is significantly influenced by the medium in which it operates. An illustration of the impact of different mediums on transportation can be observed in the case of a ship navigating through water, which experiences the buoyant force of the water, and an airship traveling through air, which encounters the effects of air medium. The relationship between static buoyancy and the density of the medium is noteworthy. Ships can leverage this phenomenon due to the fact that the density of water is significantly higher than that of air. Consequently, when compared to an airship, a ship exhibits greater lift.

Furthermore, with regards to energy, there exist concepts pertaining to slow cycle carbon and fast cycle carbon. The slow cycle of carbon refers to a carbon cycle mechanism that necessitates an extended duration of carbon compound retention beneath the earth's surface. The temporal span of the transformation from fossil to atmospheric CO_2 and its eventual sequestration back into the earth is on the order of thousands of years. Fast cycle carbon has a negligible impact on the climate due to its rapid processing, akin to the photosynthetic process in plants. Carbon dioxide is absorbed by a certain entity, which is subsequently consumed by living organisms. Carbon dioxide generated by living organisms, such as cows, will be reabsorbed to sustain plant life. The argument that humans produce a greater amount of CO_2eq than cars cannot be generalized due to the differing carbon cycles through which each of them passes. Specifically, humans participate in the fast carbon cycle, while cars participate in the slow carbon cycle. Direct comparison can be made between cars and buses.

The present illustration depicts a comparison between private vehicles and public transportations. This paper has demonstrated that public transportation is typically a more effective means of transporting individuals due to its greater capability to transport passenger, reduced energy consumption, and lower per-passenger carbon dioxide equivalent emissions. With the development of electric vehicles, they have emerged as a viable alternative to buses, offering comparable effectiveness. Nevertheless, this solution does not effectively address additional issues, such as heavy traffic on roads. When comparing cars to buses, it can be argued that buses are generally superior, particularly when they are powered by electricity.

Therefore, it is imperative to consider additional significant variables and thoroughly evaluate them in relation to specific requirements. The Karman-Gabrielli diagram provides guidance to transportation users in selecting suitable modes of transportation that align with their specific needs.

The evolution of transportation is contingent upon the demands of humanity within their respective eras. Developing a mode of transportation that can efficiently distribute a substantial amount of payload without requiring human involvement is deemed preferable. From an economic perspective, the potential for increased profits arises due to the efficient distribution of goods at a reduced operating cost. The delineated boundaries of compromise as depicted in all diagrams don't have a physical limit and are contingent solely upon the optimal technology available at present. As technology progresses, these boundaries will undergo continuous modification.

6.2   Recommendations

If more and more different kinds of cars are examined, Karman-Gabrielli diagrams will be even more useful. Because the compromise line on the Karman-Gabrielli diagram is dependent on the technology available at the moment and changes over time as technology advances, the Karman-Gabrielli diagram should always be updated.

Calculations of emissions may also be created in terms of the infrastructure needed to support the operation of the vehicle. For instance, an airplane that needs a runway or airport to function can also determine the emissions produced by the airport.

List of References

ACADEMIC, 2023. *Norwegian Spirit*. In: Academic Dictionaries and Encyclopaedias.
Available from: https://en-academic.com/dic.nsf/enwiki/754410
Archived at: https://perma.cc/XM76-A49Y

ACKERT, Shannon, 2013. *Aircraft Payload-Range Analysis for Financiers.* Aircraft Monitor.
Available from: https://bit.ly/3ZYYbGz
Archived at: https://perma.cc/LL7U-7ZW3

AS, 2023. *ASW 28*. Poppenhausen: Alexander Schleicher Segelflugzeugbau.
Available from: https://www.alexander-schleicher.de/en/flugzeuge/asw-28/
Archived at: https://perma.cc/EPV2-TECJ

BANKS, W.F., 1977. *Prospects for energy conservation in the pipeline industry*. La Jolla,
CA: Systems, Science and Software, 1977-11-30. Report: Task 4 and 5, Contract: EY-76-C-03-1171, Department: Department of Energy.
Available from: https://doi.org/10.2172/6303555

BERDOWSKI, Z., et al., 2009. *Survey on Standard Weights of Passengers and Baggage*.
Zoetermeer: EASA.
Available from: https://bit.ly/3oneFu7
Archived at: https://perma.cc/64XT-BUJD

BRAIN, Marshall, ADKINS, Brian, 2023. *How Gliders Work.* In: How Stuff Works.
Available from: https://bit.ly/3JtWl9n
Archived at: https://perma.cc/6G4U-CGZC

BRITANNICA, 2023. *Airship.* In: Encyclopedia Britannica.
Available from: https://www.britannica.com/technology/airship
Archived at: https://perma.cc/M3ZE-TS9T

BUNDLE, Armin, 2018. *Simulation of a Solar Airship.* Master Thesis. Erlangen: Friedrich-Alexander-Universität Erlangen-Nürnberg.
Available from: https://bit.ly/42ui363
Archived at: https://perma.cc/X6BY-QB53

CAREXPERT, 2023. *About the 2019 Mercedes-Benz G-Class 63*. CarExpert Pty Ltd.
Available from: https://www.carexpert.com.au/mercedes-amg/g/2019-63-c537427c
Archived at: https://perma.cc/YL4G-JJXJ

CODE 7700, 2023. *L/Dmax.* In : Code 7700 LLC.
Available from: https://code7700.com/l_over_d_max.htm
Archived at: https://perma.cc/SCY6-ZKSJ

COLLINS, 2023a. *Energy Consumption*. In: Collins Dictionaries.
Available from: https://bit.ly/41kwBnQ

COLLINS, 2023b. *Cruising Speed*. In: Collins Dictionaries.
Available from: https://bit.ly/41BgDVV

COLLINS, 2023c. *Bulker*. In: Collins Dictionaries.
Available from: https://www.collinsdictionary.com/dictionary/english/bulker

COLLINS, 2023d. *Tanker*. In: Collins Dictionaries.
Available from: https://www.collinsdictionary.com/dictionary/english/tanker

COLLINS, 2023e. *Container Vessel*. In: Collins Dictionaries.
Available from: https://bit.ly/3KP1LwB

COLLINS, 2023f. *Comparing*. In: Collins Dictionaries.
Available from: https://www.collinsdictionary.com/dictionary/english/compare

COLLINS, 2023g. *Mode of Transport*. In: Collins Dictionaries.
Available from: https://bit.ly/3L6rCBq

COLLINS, 2023h. *Mode of Transportion*. In: Collins Dictionaries.
Available from: https://bit.ly/3L6rCBq

COLLINS, 2023i. *Means of Transport*. In: Collins Dictionaries.
Available from: https://bit.ly/3L8BSsI

COLLINS, 2023j. *Imporoved*. In: Collins Dictionaries.
Available from: https://www.collinsdictionary.com/dictionary/english/improved

CONCA, James, 2014. *Pick Your Poison for Crude – Pipeline, Rail, Truck or Boat*. In: Forbes, 2014-04-26.
Available from: https://bit.ly/40bQhZy
Archived at: https://perma.cc/K8ZM-BKKN

CRA, 2023. *Corel Reefs 101 – Global Threats to Coral Reefs.* San Francisco, CA, USA: Coral Reef Alliance.
Available from: https://coral.oeg/en/coral-reefs-101/global-threats
Archived at: https://perma.cc/HL38-DR27

DANKANICH, Andrew, PETERS, David, 2017. *Turbofan Engine Bypass Ratio as a Function of Thrust and Fuel Flow.* Final Report. St. Louis: Washington University.
Available from: https://doi.org/10.7936/gps1-kd93

DEUTSCHE BAHN, 2023. *Get to Your Destination with Renewable Power*. Deutsche Bahn AG.
Available from: https://nachhaltigkeit.deutschebahn.com/en/measures/ice
Archived at: https://perma.cc/Q2YK-J5M6

EBERT, Mark, MOORE-COLYER, Mariel J S., 2020. *The Energy Requirements of Performance Horses in Training.* In: Translational Animal Science, vol. 4, no. 2, pp. 569-588
Available from: https://doi.org/10.1093/tas/txaa032

ECOMODDER, 2018. *Vehicle Coefficient of Drag List*.
Available from: https://ecomodder.com/wiki/Vehicle_Coefficient_of_Drag_List
Archived at: https://perma.cc/G7GU-TCUY

ENGHEIM, Erik, 2018. *Calculating Lifting Capacity of Airships.* Medium.
Available from: https://bit.ly/41iY35l
Archived at: https://perma.cc/7T9Y-NBM4

EUROCOPTER, 2007. *EC120 B Technical Data*. Eurocopter an EADS Company.
Available from: https://bit.ly/40scGCc
Archived at: https://perma.cc/2VJ9-QSFK

EUROCOPTER, 2009. *AS350 B3 Technical Data*. Eurocopter an EADS Company.
Available from: https://bit.ly/43GuKv5
Archived at: https://perma.cc/82ZJ-3DUB

EV DATABASE, 2021. *Tesla Model 3*. Electric Vehicle Database.
Available from: https://bit.ly/41EX7Ij
Archived at: https://perma.cc/PG46-PGSL

EV DATABASE, 2022. *Audi E-Tron 55 Quattro*. Electric Vehicle Database.
Available from: https://ev-database.org/car/1355/Audi-e-tron-55-quattro
Archived at: https://perma.cc/NL8L-DAC9

FAA, 2023. *Aerodynamics of Flight*. In: Pilot's Handbook of Aeronautical Knowledge. Oklahoma City: United States Department of Transportation, pp. 5-1 – 5-51.
Available from: https://bit.ly/3sDDc00
Archived at: https://perma.cc/WUX4-S2CL

FRITZ, E., BLOW, L. KLUHSPIES, J., KIRCHER, R., WITT, M.H., 2018. *Energy Consumption of Track-Based High-Speed Trains: Maglev Systems in Comparison with Wheel-Rail Systems*. In: Transportation System and Technology, vol. 4, no. 3, pp. 134-155.
Available from: https://doi.org/10.17816/transsyst201843s1134-155

GARD.NO, 2012. *Tonnage Measurement of Ships*. In : Insight, 2012-10-24, no. 208.
Available from: https://bit.ly/3Jxx2Dr
Archived at: https://perma.cc/X4UJ-5W9Y

GABRIELLI, Giuseppe, VON KARMAN, Theodore, 1950. *What Price Speed? Specific Power Required for Propulsion of Vehicles*. In: Mechanical Engineering, vol. 72, no. 2, pp. 775-781.
Available from: https://stanford.io/48b0ZEP
Archived at: https://perma.cc/5FZH-YGTR.

GÖß, Simon, 2017. *Tutorial Gasmarkt Teil 6: Erdgastransport und -speicherung*. Energy Brainpool GmbH & Co. KG.
Available from: https://bit.ly/40jJ2im
Archived at: https://perma.cc/J4BL-NCAK

GROSSMAN, Dan, 2017a. *Hindenburg Flight Operations and Procedures.* Airships.net.
Available from: https://bit.ly/400jNlS
Archived at: https://perma.cc/C7ST-D8MY

GROSSMAN, Dan, 2017b. *Hydrogen and Helium in Rigid Airship Operations.* Airships.net.
Available from: https://bit.ly/41IvNsJ
Archived at: https://perma.cc/H97Y-QVPV

GULANI, Schaugar Taher, 2022. Proposing a Classification for Aeronautics, Astronautics and Aerospace Sciences. Bachelor Thesis. Hamburg: Hochschule für Angewandte Wissenschaften Hamburg.
Available from: https://www.fzt.haw-hamburg.de/pers/Scholz/arbeiten/classification
Archieved at: https://perma.cc/F2XM-TF8L

HAMMAMI, Mohamed Oussama, 2021a. *Turbofan Specific Fuel Consumption, Size and Mass from Correlated Engine Parameters* (Excel File). Hochschule für Angewandte Wissenschaften Hamburg.
Available from: https://doi.org/10.7910/DVN/UW6FAP

HAMMAMI, Mohamed Oussama, 2021b. *Turbofan Specific Fuel Consumption, Size and Mass from Correlated Engine Parameters* (Presentation). Hochschule für Angewandte Wissenschaften Hamburg.
Available from: https://bit.ly/3sETq9e
Archived at: https://perma.cc/M46R-4BQR

HERZ, Rolf, 2004. *Grundlagen der Rohrleitungs- und Apparatetechnik*. Essen: Vulkan-Verlag, pp. 180.
Available from: https://bit.ly/44GJKIy (Closed Access)
Archived at: https://perma.cc/Z5SR-7RD7

HIGHSKYFLYING, 2023. *Can a Helicopter Glide If the Engine Fails?*.
Available from: https://www.highskyflying.com/can-helicopters-glide/
Archived at: https://perma.cc/3V2B-LTXA

JENKINSON, L., SIMPKIN, P., RHODES, D., 2001. *Aircraft Data File*. Butterworth-Heinemann.
Available from: https://bit.ly/41nRBKg
Archived at: https://bit.ly/3mGwNia

KMET, Jaroslav, 2022. *The Impact of Frontal Area on Vehicle Propulsion Energy Consumption.* In: LinkedIn, 2022-02-28.
Available from: https://bit.ly/3mLacRt
Archived at: https://perma.cc/3QL3-PX2G

KOLLMAR, Dirk, 2023. *Betrieb von Kreiselpumpen* (Presentation). Frankenthal: KSB AG, pp. 17.
Available from: https://bit.ly/43J1ZxW
Archived at: https://perma.cc/9L57-ZHRV

KRISTENSEN, Hans Otto, 2017a. *Prediction of Resistance and Propulsion Power of Ships.* Report. Technical University of Denmark.
Available from: https://bit.ly/3JuR4OU
Archived at: https://perma.cc/3QET-B4YD

KRISTENSEN, Hans Otto, 2017b. *Ship-Desmo.* Report. Technical University of Denmark.
Available from: https://bit.ly/40k42Wa
Archived at: https://doi.org/10.7910/DVN/INTM5L

KÜCHEMANN, Dietrich, 2012 [1978]. *The Aerodynamic Design of Aircraft AIAA Education Series*. Reston, VA: American Institute of Aeronautics & Astronautics.
Available from: https://bit.ly/3UHUXW3
Archived at: https://perma.cc/45CN-TEPN

LETADLANAPLATNE, 2023. *LZ 129 Hindenburg*.
Available from: https://bit.ly/3L8FN98
Archived at: https://perma.cc/9AHD-ML3Q

MUSK, Elon, 2013. *Hyperloop*. Austin, TX, USA: Tesla, 2013-08-12.
Available from: https://www.tesla.com/blog/hyperloop
Archived at: https://perma.cc/UZ62-KNBZ

MCKENZIE, Richard B., 2013. *Why Walking to Work Can be More Polluting Than Driving to Work*. Econlib.
Available from: https://bit.ly/3US7KoP
Archived at: https://perma.cc/E528-R3K4

MERCEDES-BENZ, 2019. *News 2019.* In: Cyprus Import Corporation Ltd (CiC).
Available from: https://bit.ly/43KXNOe
Archived at: https://perma.cc/KJ2F-6NDG

MERCEDES-BENZ, 2023. *Technical Data at a Glance.* Daimler Truck AG.
Available from: https://bit.ly/3mBB32p
Archived at: https://perma.cc/Q5K8-MTT5

MERIAM-WEBSTER, 2023a. *Payload*. In: Meriam-Webster Dictionaries.
Available from: https://www.merriam-webster.com/dictionary/payload

MERIAM-WEBSTER, 2023b. *Figure of Merit*. In: Meriam-Webster Dictionaries.
Available from: https://bit.ly/3L5r3aV

NASA, 2023. *Glide Slope Ratio*.
Available from: https://bit.ly/3lr2uv1
Archived at: https://perma.cc/4SJJ-G7XF

NCL, 2023. *Wie Viele Koffer Darf Ich Mitnehmen?*. In: Norwegian Cruise Line Holdings Ltd.
Available from: https://bit.ly/40jILvR
Archived at: https://perma.cc/MV5W-DYB9

OAK RIDGE LABORATORY, 2023a. *2017 Toyota Prius*. In: Oak Ridge National Laboratory.
Available from: https://bit.ly/3GTKYXM
Archived at: https://perma.cc/W5EC-RRGH

OAK RIDGE LABORATORY, 2023b. *2020 Mercedes-Benz G-Class*. In: Oak Ridge National Laboratory.
Available from: https://bit.ly/3A7beu3
Archived at: https://perma.cc/33KV-NT66

ROBINSON, 2022. *R44 RAVEN II & CLIPPER II*. Torrance: Robinson Helicopter Company.
Available from: https://robinsonheli.com/r44-raven-ii-clipper-ii-helicopters/
Archived at: https://perma.cc/VJ6A-3SL8

SCANIA, 2023. *Specification of Scania P380CB-6x4.*
Available from: https://bit.ly/41sUaue
Archived at: https://perma.cc/W4F4-9ER8

SCHOLZ, Dieter, 2015. *Aircraft Design.* Lecture Notes. Hamburg University of Applied Science.
Available from: http://LectureNotes.AircraftDesign.org

SCHOLZ, Dieter, 2019. *Limits to Principles of Electric Flight.* Presentation. Deutscher Luft- und Raumfahrtkongress (Darmstadt, Germany, 30.09.-02.10.2019)
Available from: https://doi.org/10.5281/zenodo.4072283

SCHOLZ, Dieter, 2021. *Umweltschutz in der Luftfahrt – Hintergründe und Argumente zur aktuellen Diskussion*. Bericht. Hochschule für Angewandte Wissenschaften Hamburg, Aircraft Design and Systems Group (AERO).
Available from: https://doi.org/10.48441/4427.225

SCHOLZ, Dieter, 2022a. *Drag Estimation*. Lecture Notes. Hochschule für Angewandte Wissenschaften Hamburg.
Available from: https://purl.org/aero/M2022-10-28
Archived at: https://bit.ly/45HHL87

SCHOLZ, Dieter, 2022b. *Flugmechanik – Flugleistung und statische Stabilität der Längsbewegung.* Lecture Notes. Hochschule für Angewandte Wissenschaften Hamburg.
Available from: http://SkriptFlugmechanik.ProfScholz.de

SCHUMANN, Ulrich, 2002. *Aircraft Emissions.* In: MUNN, Ted, ed. Encyclopedia of Global Environmental Change, vol.3, Causes and Consequences of Global Environmental Change. Chichester, UK: John Wiley & Sons, pp. 178-186.
Available from: https://bit.ly/3A9Dv34
Archived at: https://perma.cc/8D4D-X6FG

SHACMAN, 2020. *China 40 Ton Dump Truck, Chinese 40 Ton Tipper Truck, 40 Ton Dumper Truck*.
Available from: https://bit.ly/3GSAWpM
Archived at: https://perma.cc/A7MZ-YMFA

SHIP TECHNOLOGY, 2015. *Britannia Cruise Ship*. In: Ship Technology. London, UK: Verdict Media, 2015-04-02.
Available from: https://bit.ly/3KIJ8u5
Archived at: https://perma.cc/7RKZ-PPE5

SHIPS HUB, 2019. *The Newest Liner Britannia*.
Available from: https://bit.ly/3KIJi4F
Archived at: https://perma.cc/BAZ7-EWVJ

THE RAILWAY RESEARCH GROUP, 2005. *What Price Speed – Revisited*. In: Ingenia, 2005-03-22.
Available from: https://bit.ly/3LgrsH6
Archived at: https://perma.cc/43XQ-BJRW

TEITLER, S., PROODIAN, R.E., 1980. *'What price speed', revisited*. Reston, VA: Aerospace Research Central, 2012-05-23, vol. 4, no. 1.
Available from: https://doi.org/10.2514/3.48016

TRANCOSSI, Michele, 2016. *What Price Speed? A Critical Revision Through Constructal Optimization of Transport Modes*. In: International Journal of Energy and Environmental Engineering, vol. 7 (2016), pp. 425-448.
Available from: https://doi.org/10.1007/s40095-015-0160-6
Archived at: https://perma.cc/4P8B-TV5Z

TRANSPORT ENVIRONMENT, 2023. *Greenhouse Gases*. European Federation for Transport and Environment AISBL.
Available from: https://bit.ly/41iCrWz
Archived at: https://perma.cc/38T2-S2ZE

UTAH SOARING ASSOCIATION, 2019. *Grob 103 Twib Astir, 8485W, Performance Summary and User Documents*. Mapleton, UT, USA: Utah Soaring Association.
Available from: https://utahsoaring.org/grobn8485w/
Archived at: https://perma.cc/Q8NY-XYS8

U.S. EPA, 2021. *Control of Air Pollution From Airplanes and Airplane Engines: GHG Emission Standards and Test Procedures*. In: Federal Register, vol. 86, no. 6, pp. 2136-2174. Document Citation: 86 FR 2136FR 2136. 2021-11-01. USA: Environmental Protection Agency.
Available from: https://www.federalregister.gov/d/2020-28882
Archived at: https://perma.cc/9TAX-DALD

WAGNER, Hermann-Friedrich, 2017. *Pipelines und Tanker*. In: Welt der Physik. Bad Honnef: Deutsche Physikalische Gesellschaft 2017-08-16.
Available from: https://bit.ly/3MQapNI
Archived at: https://perma.cc/E5G9-WY9H

WEBFLEET, 2020. *So Viel Kraftstoff Verbrauchen LKW*. In: Webfleet. Leipzig: Bridgestone Mobility Solutions, 2020-02-28.
Available from: https://bit.ly/3mDCEEW
Archived at: https://perma.cc/G7MG-EG3F

WIKIPEDIA, 2023a. *Mode of Transport*.
Available from: https://en.wikipedia.org/wiki/Mode_of_transport
Archived at: https://perma.cc/M77F-6B8U

WIKIPEDIA, 2023b. *Means of Transport*.
Available from: https://en.wikipedia.org/wiki/Means_of_transport
Archieved at :   https://perma.cc/7WEW-RW7G

WIKIPEDIA, 2023c. *Diagramme de Gabrielli – von Karman*.
Available from: http://bit.ly/401Aq0e
Archived at: https://perma.cc/7NM5-P3L3

WIKIPEDIA, 2023d. *Lift-to-Drag Ratio*.
Available from: https://en.wikipedia.org/wiki/Lift-to-drag_ratio
Archived at: https://perma.cc/FJ8M-B2VF

WIKIPEDIA, 2023e. *Rolling Resistance*.
Available from: https://en.wikipedia.org/wiki/Rolling_resistance
Archived at: https://perma.cc/HNQ3-76SS

WIKIPEDIA, 2023f. *Energy Efficiency in Transport.*
     Available from: https://en.wikipedia.org/wiki/Energy_efficiency_in_transport
     Archived at: https://perma.cc/TC4B-PPYN

WIKIPEDIA, 2023g. *Hyperloop*.
     Available from: https://de.wikipedia.org/wiki/Hyperloop
     Archived at: https://perma.cc/TE6J-8UP2

WIKIPEDIA, 2023h. *Queen Mary 2*.
     Available from: https://bit.ly/3V01jAl
     Archived at: https://perma.cc/CJU2-VKKR

WIKIPEDIA, 2023i. *Toyota Prius (XW50)*.
     Available from: https://en.wikipedia.org/wiki/Toyota_Prius_(XW50)
     Archived at: https://perma.cc/PAH6-DXYA

WIKIPEDIA, 2023j. *Dienstgewicht*.
     Available from: https://bit.ly/3A4VqIe
     Archived at: https://perma.cc/5BMK-EQW5

WIKIPEDIA, 2023k. *ICE 3*.
     Available from: https://de.wikipedia.org/wiki/ICE_3
     Archived at: https://perma.cc/Z3N8-LZQK

WIKIPEDIA, 2023l. *TGV Duplex*.
     Available from: https://de.wikipedia.org/wiki/TGV_Duplex
     Archived at: https://perma.cc/WY9H-2CNT

WIKIPEDIA, 2023m. *Pareto Front*.
     Available from: https://en.wikipedia.org/wiki/Pareto_front
     Archived at: https://perma.cc/3RRL-6VEJ

WIKIPEDIA, 2023n. *Value of Time*.
     Available from: https://en.wikipedia.org/wiki/Value_of_time
     Archived at: https://perma.cc/RH3E-LWDS

All online resources have been accessed on 2023-04-19 or later.

Appendix A – Transport Figure of Merit Results

Table A.1 Transport Figure of Merit Based on Lift-to-Drag Ratio of All Vehicles

Vehicle	$a_{\left(\frac{L}{D}\right)}$
Hyperloop Alpha Passenger	111098.25
Hyperloop Alpha Passenger and Cargo	78994.20
VLBC Bulker	15314.03
Suezmax Tanker	12439.43
VLCC Tanker	12239.93
Aframax Tanker	9981.02
Capesize Bulker	9789.23
Panamax Bulker	8873.98
Post Panamax (typ.4) Container Vessel	7288.35
ICE 3	6478.21
Panamax Tanker	6339.65
P&O Britannia	6220.41
TGV Duplex	6131.25
YB-49	6062.82
Handymax Tanker	5946.42
Concorde	5940.01
A340-300	5753.06
Handymax Bulker	5686.98
Norwegian Spirit	5604.50
MD-11	5398.72
MD-11 (Cargo)	5398.72
B767-300	5247.17
B737-300	5073.26
Handysize Bulker	5067.46
B757-200	5042.71
Post Panamax (typ.3) Container Vessel	5012.99
Queen Mary 2	4941.05
A310-300	4892.72
Handysize Tanker	4773.07
B747-400	4719.83
B747-400 (Cargo)	4719.83
A300-600R	4557.28
A320-200	4538.10
A321-200	4338.49
Panamax (typ.2) Container Vessel	4295.86
Avro Vulcan	4283.45
TU-154M	4202.90
MD90-30	4124.27
Feeder Container Vessel	3863.93
Fokker 100	3744.68
Small Bulker	3313.27
Small Tanker	2950.79

ASW 28	2500.20
LZ 129 Hindenburg	1342.23
Bus Tourisimo L (City)	1234.77
Shacman (City)	1110.57
Scania P380 (City)	1103.24
Tesla 3 (City)	1048.44
Audi E-tron (City)	1022.80
Toyota Prius (City)	936.73
Active racehorse	883.60
Grob 103	865.05
Mercedes G-Class (City)	675.03
BUs Tourisimo L (Earthway)	483.15
Shacman (Earthway)	310.97
Scania P380 (Earthway)	310.63
Tesla 3 (Earthway)	307.91
Audi E-tron (Earthway)	306.55
Toyota Prius (Earthway)	301.57
Horse with Carriage, Trotting	301.08
Mercedes G-Class (Earthway)	280.56
Bicycle on Racetrack	265.60
Bicycle Speeding on Highway	253.67
R44 Raven II	227.80
R44 Raven I	214.49
Bicycle Pleasure Trip	211.96
Water pipeline	207.19
Gas pipeline	180.60
AS350 B3	173.23
EC120 B	161.29
Horse with Carriage, Fast Step	132.03
Heavy oil pipeline	88.60
100-yard Runner	81.09
Human Marching Fast	43.46
Human walking	19.80

Table A.2 Transport Figure of Merit Based on Lift-to-Drag Ratio Regarding Payload Mass of All Vehicles

Vehicle	$a_{(\frac{L}{D})pl}$
Hyperloop Alpha Passenger and Cargo	27040.32
Hyperloop Alpha Passenger	20738.34
VLBC Bulker	11681.36
Suezmax Tanker	9177.11
VLCC Tanker	9148.91
Aframax Tanker	7282.43
Capesize Bulker	7250.66
Panamax Bulker	6602.28
Post Panamax (typ.4) Container Vessel	5036.67
Panamax Tanker	4532.80

Handymax Tanker	4175.12
Handymax Bulker	4070.67
Handysize Bulker	3392.46
Handysize Tanker	3149.99
Post Panamax (typ.3) Container Vessel	2772.85
Panamax (typ.2) Container Vessel	2257.37
Small Bulker	2028.97
Feeder Container Vessel	1987.49
MD-11 (Cargo)	1749.88
Small Tanker	1742.99
B737-300	1440.13
B747-400 (Cargo)	1344.00
B767-300	1312.39
A321-200	1233.30
B757-200	1117.75
A300-600R	1098.56
A310-300	1086.18
MD-11	1057.33
A340-300	1022.18
MD90-30	1011.25
A320-200	1000.23
Fokker 100	965.33
TGV Duplex	884.09
TU-154M	756.52
B747-400	727.74
Scania P380 (City)	726.53
ASW 28	619.10
ICE 3	608.14
Shacman (City)	587.53
Avro Vulcan	555.49
Concorde	429.61
Bus Tourisimo L (City)	403.32
YB-49	312.62
Grob 103	277.76
Toyota Prius (City)	228.30
Tesla 3 (City)	215.57
Bicycle Speeding on Highway	214.02
Bicycle on Racetrack	209.06
Water pipeline (electric)	207.19
Scania P380 (Earthway)	204.56
Water pipeline (diesel/gas)	186.47
Gas pipeline (electric)	180.60
Bicycle Pleasure Trip	177.58
Shacman (Earthway)	164.51
Gas pipeline (diesel/gas)	162,54
Bus Tourisimo L (Earthway)	157.81
Audi E-tron (City)	153.07
Active racehorse	107.80

Mercedes G-Class (City)	102.42
Heavy oil pipeline (electric)	88.60
100-yard Runner	81.09
Heavy oil pipeline (diesel/gas)	79.74
AS350 B3	77.68
R44 Raven II	74.53
Toyota Prius (Earthway)	73.50
R44 Raven I	69.13
EC120 B	68.18
Tesla 3 (Earthway)	63.31
LZ 129 Hindenburg	55.31
Horse with Carriage, Trotting	52.83
Audi E-tron (Earthway)	45.88
Human Marching Fast	43.46
Mercedes G-Class (Earthway)	42.57
Queen Mary 2	27.06
P&O Britannia	26.84
Norwegian Spirit	23.96
Human walking	19.80
Horse with Carriage, Fast Step	17.54

Table A.3 Transport Figure of Merit Based on Inverse of Energy Consumption per Payload and Range of All Vehicles

Vehicle	a_E
VLBC Bulker	335.22
VLCC Tanker	318.68
Suezmax Tanker	257.00
Hyperloop Alpha Passenger and Cargo	214.49
Hyperloop Alpha Passenger	214.49
Capesize Bulker	200.19
Aframax Tanker	197.69
Panamax Bulker	187.87
Post Panamax (typ.4) Container Vessel	178.96
Panamax Tanker	154.20
Handymax Bulker	131.35
Handymax Tanker	122.38
Post Panamax (typ.3) Container Vessel	99.75
Handysize Bulker	86.57
Panamax (typ.2) Container Vessel	81.87
Handysize Tanker	81.23
MD-11 (Cargo)	68.69
Feeder Container Vessel	66.80
Scania P380 (City)	59.33
MD90-30	54.80
Shacman (City)	50.45
B747-400 (Cargo)	49.38

B767-300		48.76
Small Bulker		48.46
B737-300		46.00
ICE 3		45.56
Small Tanker		42.78
TGV Duplex		42.71
A321-200		42.25
MD-11		41.50
A340-300		40.69
A310-300		39.47
A300-600R		39.45
B757-200		38.52
A320-200		35.68
Scania P380 (Earthway)		35.60
Shacman (Earthway)		30.28
B747-400		26.74
Fokker 100		25.13
Bus Tourisimo L (City)		24.94
BUs Tourisimo L (Earthway)		24.94
Tesla 3 (City)		22.49
TU-154M		19.29
Concorde		18.26
Water pipeline (electric)		15.84
Bicycle on Racetrack		15.48
Audi E-tron (City)		14.33
Gas pipeline (electric)		13.81
Tesla 3 (Earthway)		13.49
Avro Vulcan		13.17
Bicycle Speeding on Highway		10.16
Audi E-tron (Earthway)		8.60
Toyota Prius (City)		8.45
LZ 129 Hindenburg		7.42
Heavy oil pipeline (electric)		6.77
Bicycle Pleasure Trip		6.30
Water pipeline (diesel/gas)		5.28
Toyota Prius (Earthway)		5.07
100-yard Runner		5.01
YB-49		5.00
Gas pipeline (diesel/gas)		4.60
Racehorse		4.24
R44 Raven II		3.33
R44 Raven I		3.12
AS350 B3		2.36
Mercedes G-Class (City)		2.28
Heavy oil pipeline (diesel/gas)		2.26
EC120 B		2.11
Human Marching Fast		2.01
Mercedes G-Class (Earthway)		1.37

Queen Mary 2	1.10
Horse with Carriage, Trotting	0.99
Norwegian Spirit	0.92
P&O Britannia	0.75
Human walking	0.67
Horse with Carriage, Fast Step	0.50

Table A.4 Transport Figure of Merit Based on Inverse of Primary Energy Consumption per Payload and Range of All Vehicles

Vehicle	a_Eprim
VLBC Bulker	304.74
VLCC Tanker	289.71
Suezmax Tanker	233.64
Capesize Bulker	181.99
Aframax Tanker	179.72
Panamax Bulker	170.79
Post Panamax (typ.4) Container Vessel	162.69
Panamax Tanker	140.18
Handymax Bulker	119.40
Handymax Tanker	111.26
Hyperloop Alpha Passenger and Cargo	102.14
Hyperloop Alpha Passenger	102.14
Post Panamax (typ.3) Container Vessel	90.68
Handysize Bulker	78.70
Panamax (typ.2) Container Vessel	74.43
Handysize Tanker	73.85
MD-11 (Cargo)	62.44
Feeder Container Vessel	60.73
Scania P380 (City)	53.94
MD90-30	49.82
Shacman (City)	45.87
B747-400 (Cargo)	44.89
B767-300	44.33
Small Bulker	44.06
B737-300	41.82
Small Tanker	38.89
A321-200	38.41
MD-11	37.73
A340-300	37.00
A310-300	35.88
A300-600R	35.87
B757-200	35.02
A320-200	32.44
Scania P380 (Earthway)	32.37
Shacman (Earthway)	27.52

B747-400	24.30
Fokker 100	22.85
ICE 3	21.69
TGV Duplex	20.34
TU-154M	17.54
Concorde	16.60
Bicycle on Racetrack	15.48
Avro Vulcan	11.98
Bus Tourisimo L (City)	11.88
BUs Tourisimo L (Earthway)	11.88
Tesla 3 (City)	10.71
Bicycle Speeding on Highway	10.16
Toyota Prius (City)	7.69
Water pipeline (electric)	7.54
Audi E-tron (City)	6.82
LZ 129 Hindenburg	6.75
Gas pipeline (electric)	6.57
Tesla 3 (Earthway)	6.43
Bicycle Pleasure Trip	6.30
100-yard Runner	5.01
Water pipeline (diesel/gas)	4.89
Toyota Prius (Earthway)	4.61
YB-49	4.55
Racehorse	4.24
Gas pipeline (diesel/gas)	4.18
Audi E-tron (Earthway)	4.09
Heavy oil pipeline (electric)	3.22
R44 Raven II	3.03
R44 Raven I	2.83
AS350 B3	2.15
Mercedes G-Class (City)	2.07
Heavy oil pipeline (diesel/gas)	2.05
Human Marching Fast	2.01
EC120 B	1.92
Mercedes G-Class (Earthway)	1.24
Queen Mary 2	1.00
Horse with Carriage, Trotting	0.99
Norwegian Spirit	0.84
P&O Britannia	0.68
Human walking	0.67
Horse with Carriage, Fast Step	0.50